
Research Article: Confirmation | Sensory and Motor Systems

State-Dependent Modification of Sensory Sensitivity via Modulation of Backpropagating Action Potentials

Carola Städele^{1,2}, Margaret L. DeMaegd² and Wolfgang Stein²

¹*Institute of Neurobiology, Ulm University, Ulm 89069, Germany*

²*School of Biological Sciences, Illinois State University, Normal, IL 61790, USA*

DOI: 10.1523/ENEURO.0283-18.2018

Received: 21 July 2018

Accepted: 31 July 2018

Published: 13 August 2018

Author Contributions: CS, MLD, and WS designed research. CS, MLD, and WS performed research. CS, MLD, and WS analyzed data. CS, and WS wrote the paper.

Funding: [http://doi.org/10.13039/100000001National Science Foundation \(NSF\) IOS 1354932](http://doi.org/10.13039/100000001National Science Foundation (NSF) IOS 1354932)

Funding: [http://doi.org/10.13039/501100001659Deutsche Forschungsgemeinschaft \(DFG\) STE 937/9-1](http://doi.org/10.13039/501100001659Deutsche Forschungsgemeinschaft (DFG) STE 937/9-1)

Funding: [http://doi.org/10.13039/501100001655Deutscher Akademischer Austauschdienst \(DAAD\)](http://doi.org/10.13039/501100001655Deutscher Akademischer Austauschdienst (DAAD))

Conflict of Interest: Authors report no conflict of interest.

Founding sources: This work was supported by grants from the German Research Foundation (DFG STE 937/9-1), National Science Foundation (NSF IOS 1354932), Illinois State University and The German Academic Exchange Service (DAAD).

Correspondence should be addressed to Wolfgang Stein, wstein@neurobiologie.de

Cite as: eNeuro 2018; 10.1523/ENEURO.0283-18.2018

Alerts: Sign up at eneuro.org/alerts to receive customized email alerts when the fully formatted version of this article is published.

Accepted manuscripts are peer-reviewed but have not been through the copyediting, formatting, or proofreading process.

Copyright © 2018 Städele et al.

This is an open-access article distributed under the terms of the Creative Commons Attribution 4.0 International license, which permits unrestricted use, distribution and reproduction in any medium provided that the original work is properly attributed.

- 1 **1. Manuscript Title:** State-dependent modification of sensory sensitivity via modulation of
2 backpropagating action potentials
3
- 4 **2. Abbreviated Title:** Antidromic spikes modulate sensory encoding
5
- 6 **3. Authors:** Carola Städele^{1,2,3}, Margaret L. DeMaegd² & Wolfgang Stein²
7 ¹Institute of Neurobiology, Ulm University, 89069 Ulm, Germany;
8 ²School of Biological Sciences, Illinois State University, Normal, IL 61790, USA.
9 ³present address: Department of Integrative Biology and Physiology, UCLA, Los Angeles, CA 90095-
10 7239, USA
11
- 12 **4. Author Contributions:** CS, MLD, and WS designed research. CS, MLD, and WS performed
13 research. CS, MLD, and WS analyzed data. CS, and WS wrote the paper.
14
- 15 **5. Correspondence should be addressed to:** wstein@neurobiologie.de
16
- 16 **6. Number of Figures:** 9
17
- 17 **7. Number of Tables:** 1
18
- 18 **8. Number of Multimedia:** 0
19
- 19 **9. Number of Words in Abstract:** 247
20
- 20 **10. Number of words for Significance Statement:** 119
21
- 21 **11. Number of words for Introduction:** 742
22
- 22 **12. Number of words for Discussion:** 2456
23
- 24 **13. Acknowledgements:** We would like to thank Dr. Lingjun Li for providing the Orcokininins used in this
25 study.
26
- 27 **14. Conflict of Interest:** Authors report no conflict of interest
28
- 29 **15. Founding sources:** This work was supported by grants from the German Research Foundation
30 (DFG STE 937/9-1), National Science Foundation (NSF IOS 1354932), Illinois State University and
31 The German Academic Exchange Service (DAAD).

32 ABSTRACT

33 Neuromodulators play a critical role in sensorimotor processing via various actions, including pre- and
34 postsynaptic signal modulation and direct modulation of signal encoding in peripheral dendrites. Here we
35 present a new mechanism that allows state-dependent modulation of signal encoding in sensory
36 dendrites by neuromodulatory projection neurons. We studied the impact of antidromic action potentials
37 (APs) on stimulus encoding using the anterior gastric receptor (AGR) neuron in the heavily modulated
38 crustacean stomatogastric ganglion. We found that ectopic AP initiation in AGR's axon trunk is under
39 direct neuromodulatory control by the inferior ventricular (IV) neurons, a pair of descending projection
40 neurons. IV neuron activation elicited a long-lasting decrease in AGR ectopic activity. This modulation
41 was specific to the site of AP initiation and could be mimicked by focal application of the IV neuron co-
42 transmitter histamine. IV neuron actions were diminished after blocking H₂ receptors in AGR's axon trunk,
43 suggesting a direct axonal modulation. This local modulation did not affect the propagation dynamics of
44 en-passant APs. However, decreases in ectopic AP frequency prolonged sensory bursts elicited distantly
45 near AGR's dendrites. This frequency-dependent effect was mediated via the reduction of antidromic
46 APs, and the diminishment of backpropagation into the sensory dendrites. Computational models suggest
47 that invading antidromic APs interact with local ionic conductances the rate constants of which determine
48 the sign and strength of the frequency-dependent change in sensory sensitivity. Antidromic APs therefore
49 provide descending projection neurons with a means to influence sensory encoding without affecting AP
50 propagation or stimulus transduction.

51 SIGNIFICANCE STATEMENT

52 Descending modulatory projection neurons are a hallmark of motor systems and fundamentally involved
53 in sensorimotor processing. While they have been shown to interact on many levels with motor networks
54 to dynamically and rapidly adjust motor and behavioral output, their actions on sensory neurons are not
55 well understood. We found that descending projection neurons directly modulate action potential initiation
56 in a sensory axon, diminishing the frequency of spontaneously generated ectopic action potentials that
57 propagate antidromically into peripheral sensory dendrites. Changes in the frequency of these
58 backpropagating action potentials determined the response of the sensory neuron to sensory stimuli. This

59 suggests that descending projection neurons modulate sensory encoding by altering axonal membrane
60 excitability and the frequency of antidromic action potential initiation.

61 **INTRODUCTION**

62 While precise and reliable sensory transduction is fundamental for adequate functioning of sensorimotor
63 systems, stimulus properties are not the only factors that contribute to sensory responses. Instead,
64 peripheral and central influences interact to produce the neuronal output, making the state of the system
65 and ongoing activity important contributors to stimulus-induced changes in motor output. A number of
66 mechanisms have been identified that affect sensory responses, including activity- or state-dependent
67 reduction of afferent spike amplitude (Clarac and Cattaert, 1996; Schmitz and Stein, 2000; Margrie et al.,
68 2001; Barriere et al., 2008), spike conduction block (Burrows and Matheson, 1994; Xiong and Chen,
69 2002; Lee et al., 2012), and regulation of spike initiation (Evans et al., 2003; Cropper et al., 2004). In
70 addition, neuromodulators alter the encoding of sensory information via their actions on local signal
71 processing and transmission, and action potential (AP) initiation (Katz and Frost, 1996; Birmingham,
72 2001; Birmingham et al., 2003; Mitchell and Johnson, 2003; Dickinson, 2006; Stein, 2009; Nadim and
73 Bucher, 2014). Here, we show that neuromodulators explore an additional pathway to alter sensory
74 encoding, namely via antidromic APs that invade the encoding region of sensory neurons.
75 Neuromodulators can alter axonal membrane excitability and lead to ectopic AP generation, a process
76 common to many systems and neurons, in both normal and pathological conditions (Dubuc et al., 1988;
77 Lena et al., 1993; Pinault, 1995; Cattaert et al., 1999; Waters et al., 2005; Ma and LaMotte, 2007;
78 Papatheodoropoulos, 2008; Bucher and Goillard, 2011). These ectopically generated APs functionally
79 add to already present orthodromic action potentials and correspondingly alter synaptic output (Lambe et
80 al., 2003). Ectopic APs also backpropagate towards the axon origin, carrying potentially important
81 information against the usual propagation direction. This reversal of the functional polarization of the
82 neuron has been implicated to affect encoding of incoming sensory and synaptic stimuli. For instance,
83 backpropagating APs can alter the sensitivity of sensory neurons in crayfish chordotonal organs involved
84 in posture control (Bevengut et al., 1997), in CA1 hippocampal neurons they cause long-lasting synaptic

85 depression of incoming synaptic signals, and they may contribute to memory consolidation (Bukalo et al.,
86 2013).

87 While ectopic APs can be initiated by modulators and backpropagating APs can influence stimulus
88 encoding, it remains unclear (1) whether these two processes combined exploit a functional dynamic
89 regulation of stimulus encoding, and (2) what underlying cellular properties facilitate the actions of
90 backpropagating APs on stimulus encoding. We hypothesized that axonal ectopic spiking is directly
91 controlled by neuromodulatory pathways, enabling a dynamic modulation of the processing of incoming
92 stimuli via APs that backpropagate into the stimulus encoding regions of neurons. To test our hypothesis,
93 we used the experimentally advantageous anterior gastric receptor neuron (AGR) in the crustacean
94 stomatogastric ganglion (STG). The STG houses several central pattern generators (CPGs) that are
95 regulated by descending modulatory projection neurons and control aspects of feeding (Stein et al., 2016;
96 Nusbaum et al., 2017; Stein, 2017). AGR senses the tension of the paired gastric mill muscles 1 (*gm1*)
97 when the animal chews food in its stomach. AGR's soma in the STG protrudes two several centimeter
98 long axons: one to the upstream commissural ganglia (CoG), and one to the peripheral *gm1* muscles
99 (Fig. 1A) (Combes et al., 1995; Daur et al., 2009). Part of AGR's activity repertoire is the generation of
100 low-frequency tonic ectopic APs in its central axon that occur as soon as muscle tension is low, i.e. at
101 rest, and in-between bites when bursts are not generated in the periphery (*in vivo* and *in vitro*,
102 Smarandache et al., 2008; Daur et al., 2009).

103 We show that axonal spike initiation in AGR is directly modulated by descending projection neurons that
104 control the CPGs in the STG. We found that the inferior ventricular (IV) neurons (Christie et al., 2004;
105 Hedrich and Stein, 2008), a pair of descending chemosensory projection neurons that are activated when
106 the animal encounters food as it starts the feeding process (Fig. 1A), decrease AGR's ectopic spike
107 frequency. This effect was mediated via release of histamine, one of the IV neuron co-transmitters, and
108 specific to the ectopic spike initiation zone (SIZ) in AGR's axon. The change in ectopic spike frequency
109 affected AGR's sensory burst via antidromic AP propagation into the sensory dendrites, with lower
110 frequencies allowing for stronger sensory bursts. Therefore, an activation of chemosensory pathways
111 primes the proprioceptive system by increasing its sensitivity to muscle tension. We thus demonstrate that

112 frequency regulation of backpropagating ectopic APs by modulatory neurons represents a mechanism to
113 alter sensory encoding.

114 MATERIALS AND METHODS

115 *Dissection*

116 Adult male crabs (*Cancer borealis*) were purchased from The Fresh Lobster Company (Gloucester, MA)
117 and kept in tanks with artificial sea water (salt content $\sim 1.025\text{g/cm}^3$, Instant Ocean Sea Salt Mix,
118 Blacksburg, VA) at 11°C and a 12-hour light-dark cycle. Before dissection, animals were anesthetized on
119 ice for 20-40 minutes. All experiments were performed *in vitro* on isolated nervous systems. The
120 stomatogastric nervous system including the supraesophageal ganglion (brain, Fig. 1A) was isolated from
121 the animal following standard procedures, pinned out in a silicone lined (Sylgard 184, Dow Corning) petri
122 dish and continuously superfused (7-12 ml/min) with physiological saline ($10\text{-}12^\circ\text{C}$). Experiments were
123 performed on fully intact and decentralized preparations. In the latter, the CoGs were removed by
124 transecting the paired *ion* and *son* nerves.

125 *Solutions*

126 *C. borealis* saline was composed of (in mM) 440 NaCl, 26 MgCl_2 , 13 CaCl_2 , 11 KCl, 11.2 Trisma base, 5
127 Maleic acid, pH 7.4-7.6 (Sigma Aldrich). In some experiments, low Ca^{2+} saline was used to block
128 chemical transmission in the posterior part of the *stn* (close to the STG neuropil). Low Ca^{2+} saline was
129 composed of (in mM) 440 NaCl, 11 KCl, 26 MgCl_2 , 0.1 CaCl_2 , 11.2 Trisma base, 5.1 Maleic acid, 12.9
130 MnCl_2 , pH 7.4-7.5. High-divalent saline ("HiDi") was used to raise spike threshold and contained 5 times
131 the amount of Ca^{2+} and Mg^{2+} than the regular saline. HiDi was composed of (in mM) 439 NaCl, 130
132 MgCl_2 , 64.5 CaCl_2 , 11 KCl, 12.4 Trisma base, 5 Maleic acid. HiDi was superfused to the posterior half of
133 the *stn* including the STG neuropil. In these experiments, AGR spike activity was monitored extracellularly
134 on the anterior part of the *stn* (close to the *stn/son* junction) which was not affected by HiDi application.
135 High K⁺ saline was composed of (in mM) 110-220 KCl, 341-231 NaCl, 26 MgCl_2 , 13 CaCl_2 , 11.2, Trisma
136 base, 5 Maleic acid, pH 7.4-7.6.

137 Modulators and Antagonists

138 Neuromodulators and antagonists were stored as concentrated stock solutions in small quantities at -
139 20°C. Immediately before an experiment, neuromodulators were diluted in saline to the desired
140 concentration. Concentrations varied between neuromodulators and are stated in the text/figures.
141 Histamine dihydrochloride (H7250, Sigma Aldrich) and FMRF-like peptide F1 (TNRNFLRF-NH₂, Bachem)
142 were diluted in ultrapure water (18.3 MΩ). Cimetidine hydrochloride (PHR1089, Sigma Aldrich) was
143 dissolved in dimethyl sulfoxide (DMSO) and protected from light throughout the length of the experiment.
144 The two Orcokininins ([Ala¹³] and [Val¹³] orcokinin, Li et al., 2002) were a gift from Dr. Lingjun Li (University
145 of Wisconsin at Madison, WI, USA).

146 Extracellular recordings

147 If not stated otherwise, all experiments were carried out using non-desheathed nervous system
148 preparations and extracellular recording techniques because removing the sheath of the STG influences
149 modulation of AGRs ectopic spiking (Goldsmith et al., 2014; Städele and Stein, 2016). For extracellular
150 recordings, petroleum jelly-wells were built to electrically isolate a small part of the nerve from the
151 surrounding bath. One of two stainless steel wires was placed inside the well to record neuronal activity of
152 all axons projecting through a particular nerve. The other wire was placed in the bath as reference
153 electrode. Extracellular signals were recorded, filtered and amplified through AM Systems amplifier
154 (Model 1700, Carlsborg, WA). Files were recorded, saved and analyzed using Spike2 Software (CED,
155 UK) at 10 kHz. The activity of AGR was monitored on multiple extracellular recordings simultaneously,
156 namely on the *stn*, *dgn*, and the *son* (Fig. 1A). AGR activity was measured as instantaneous firing
157 frequency (ff.) as determined by the reciprocal of the interspike interval.

158 Extracellular axon stimulation

159 We used retrograde extracellular nerve stimulation to activate sensory modalities of interest as described
160 in detail by Städele and colleagues (Städele et al., 2017). In short, a petroleum jelly well was built around
161 a nerve containing the axons of the neurons of interest. One of two stainless steel wires was placed
162 inside the compartment, the other was placed outside. Current pulses were applied with a Master-8 pulse

163 stimulator (A.M.P.I., Israel) controlled by self-programmed Spike2 scripts. IV neurons were activated via
164 extracellular stimulation of the *ivn* with 10 consecutive stimulus trains, 10 to 50 Hz stimulation frequency,
165 6 sec stimulus trains, 6 sec intertrain intervals, 1ms pulse duration, 0.5 to 2 Volt stimulation voltage (in
166 accordance to their *in vivo* firing pattern; Hedrich et al., 2009; Hedrich et al., 2011). The VCNs were
167 activated via extracellular stimulation of the paired *dpon* with 10 consecutive stimulus trains, 15 Hz
168 stimulation frequency, 6 sec stimulus trains, 4 sec intertrain intervals, 1ms pulse duration, 2-3 Volt
169 stimulation voltage (Beenhakker et al., 2004). In all experiments both *dpons* were stimulated
170 simultaneously using different channels on the Master-8 stimulator.

171 To determine history-dependent changes in spike conduction velocity and differences in spike failures
172 before and during IV neuron modulation, AGR was stimulated on the *agn*, a side branch leaving the *dgn*
173 that exclusively contains the AGR axon. To determine changes in spike conduction velocity we used 5
174 consecutive trains of 15 Hz stimulation frequency, each train with 28 pulses, 6 to 9 sec intertrain interval
175 and 1ms pulse duration. To elicit spike failures, the *agn* was stimulated with 10 consecutive trains, 10 to
176 50 Hz stimulation frequency (10 Hz intervals), 9 sec stimulus trains, 9 sec intertrain intervals, 1ms pulse
177 duration and 0.5 to 1 Volt before and during IV neuron stimulation. We found that the IV neuron mediated
178 decrease in AGR firing frequency was strongest after the 5th stimulation train (Fig. 1C). We thus started
179 *agn* stimulation after the 5th IV stimulation train to ensure sufficient modulation of the AGR axon. AGR
180 spike conduction velocity was calculated using standard protocols (DeMaegd et al., 2017). To assess the
181 effects of ectopic spike frequency on AGR's sensory encoding, ectopic APs were elicited via extracellular
182 stimulation of the AGR in the posterior *stn*. A minimum of 20 ectopic APs were elicited and stimulation
183 continued until the first orthodromic spike was detected. Stimulation frequencies were 10 Hz to 3 Hz in 1
184 Hz steps. Stimulus parameters were 1 ms for pulse duration and 0.2 to 1 V for stimulus amplitudes.

185 ***Drug and saline applications***

186 Neuromodulators, antagonists, HiDi and Ca²⁺ saline were applied selectively to the posterior part of the
187 *stn* where AGR's ectopic SIZ is located (Städle and Stein, 2016). A petroleum-jelly well was used to
188 isolate the application site from the rest of the nervous system. The well had an inner diameter of
189 approximately 300-400 μ m. Solutions were cooled to 10-12°C and manually applied into the well using a

190 1 ml syringe with an injection needle. To exclude temperature-induced changes in AGR frequency, saline
191 with the same temperature as the neuromodulators/antagonists was applied 5 minutes before each
192 application. Measurements for quantitative analysis were taken in steady-state (5 minutes after
193 neuromodulator/antagonist wash in). Modulators were washed out for 20 to 40 minutes with continuous
194 superfusion of cooled saline.

195 **Sensory Burst induction**

196 Either muscle stretch or high K^+ saline was used to excite AGR's peripheral dendrites and elicit sensory
197 bursts. In experiments where muscle stretch was used, the gm1 muscles and their innervation by AGR was
198 left intact. The anterior ossicles where the gm1 muscles attach to the carapace were pinned in place and
199 the posterior ossicles of the gm1 muscles were attached to an electrical micromanipulator (PatchStar,
200 Scientifica). Initial muscle stretch was set by adjusting the distance between the posterior and anterior
201 ossicle to the original muscle length measured in the intact animal before dissection. Muscle stretch was
202 applied via a ramp-and-hold movement of the manipulator. Stretch amplitude was adjusted for each
203 animal to activate AGR at physiologically relevant frequencies (typically $\sim 500\mu\text{m}$). To prevent muscle
204 damage due to many repeats and long duration experiments, muscles stretches were kept short, with a
205 holding phase of $\sim 500\text{ms}$. Stretch rate was $\sim 200\mu\text{m/s}$.

206 In experiments where high K^+ saline was used, an oblong petroleum jelly well with inner diameter of about
207 $9\times 3\text{ mm}$ was used to isolate the *agn*. Chilled physiological saline was continuously superfused into the
208 well. Inflow and outflow were placed on either side of the *agn*, such that saline flowed in one direction
209 across the *agn*. High K^+ saline was added to this flow by puffing it into the well for 0.1 to 0.5 seconds
210 using a picospitzer. To prevent accumulation of modulator effects puffs occurred every 60 to 90 seconds
211 with continuous washouts in between puffs.

212 Across preparations peripheral bursts triggered by the same concentration of high K^+ saline were quite
213 variable in burst duration and intraburst firing frequency. Thus, to reduce this variability the K^+
214 concentration was determined separately for each preparation. Specifically, K^+ saline was applied to the
215 *agn*, and changes in AGR spike frequency were measured on the *dgn*. Puffs started with the lowest
216 concentration (110mM) and K^+ concentration was increased until no further increase in intraburst firing

217 frequency could be observed. After this, the duration of the puff was adjusted so that bursts reflected
218 AGR's physiological response to muscle tension. Intraburst firing frequency was defined as the number of
219 spikes per burst - 1, divided by the burst duration.

220 To determine the influence of stimulation induced antidromic APs ('siAPs') on sensory encoding, the
221 duration of the burst, average intraburst firing frequency, and number of spikes per burst were quantified
222 following different siAP frequencies. SiAP frequencies were randomized in each preparation. In each trial,
223 siAP stimulation ended when the first AP of the sensory burst was detected. For each preparation and
224 frequency two trials were averaged in muscle stretch experiments and between one and three trials per
225 were averaged in high K⁺ saline experiments. Burst duration was measured as the time from the first
226 orthodromic AP to the last orthodromic AP. Orthodromic APs were identified by spike shape and direction
227 of propagation. Average intraburst firing frequency was determined as the average of instantaneous spike
228 frequencies during the burst.

229 **Computer Model**

230 To determine the influence that varying ectopic AP frequencies have on sensory bursts, we created a
231 model neuron with standard morphology and passive properties (Ekeberg et al., 1991) using *MadSim*
232 (Stein and Ausborn, 2004; Straub et al., 2004; Städele et al., 2015) (freely available for download at
233 <http://www.neurobiologie.de>). Passive parameters used were: leak conductance, 3 nS, C_m, 0.8 nF, resting
234 potential, -60 mV. Active membrane properties were implemented according to modified Hodgkin-Huxley
235 equations (Ausborn et al., 2007; Daur et al., 2012). The model can be found on ModelDB (accession
236 number 244260).

237 A slow K⁺ current (I_{Ks}) was implemented as non-inactivating current using $I = \bar{g} \alpha^*(V - E)$. V is the
238 membrane potential, E the K⁺ equilibrium potential (-80mV), and \bar{g} the maximum conductance. \bar{g} was set
239 to 0.7 μ S. Activation α was calculated using $\alpha = 1 / (1 + \exp((V - V_0) / s))$, with V₀ = -39.5 mV and S = -8 mV. The
240 time constant of activation was constant and varied between models (0.25 sec to 4 sec). Ectopic APs
241 were elicited with 10 ms current pulses (50 nA) at frequencies between 3 and 7 Hz. Sensory bursts were
242 elicited with 12 nA ramp-and-hold current injections (1 sec ramp up, 0.5 sec holding phase, 2 sec ramp
243 down). Simulations produced 20 s long voltage waveforms.

244 **Experimental Design and Statistical Analysis**

245 All experiments were performed on wild caught male *C. borealis*. Animals were kept for at least 7 days in
246 artificial sea water tanks prior to experiments. AGR firing frequency represents the mean instantaneous
247 firing frequency of APs occurring over 20 to 40 seconds. 'Baseline' refers to AGR firing frequency at rest,
248 while 'control' refers to AGR's firing frequency immediately before a treatment. Data were analyzed using
249 scripts for Spike2 (available on www.neurobiologie.de/spike2) and by using built-in software functions. To
250 determine temporal differences in spike appearance on multiple recording sites, a voltage threshold was
251 used for spike detection and the subsequent maximum or minimum voltage deflection of the signal
252 passing through this threshold was used as trigger. In cases where extracellular stimulus artifacts or the
253 APs of other neurons obscured the neuron of interest, obscuring signals were eliminated from recordings
254 by subtracting the average stimulus artifact with Spike2. Statistical tests were performed using SigmaStat
255 (Systat Software GmbH, Erkrath, Germany) Kolmogorov-Smirnov test with Lillifors correction was used to
256 assess normal distribution of data sets. Paired t-test and one way repeated measure ANOVA with Holm-
257 Sidak posthoc or Student-Newman-Keuls posthoc test were used to test for significant differences.
258 Statistical results are reported as followed:

- 259 • Paired t-test: $t(\text{degrees of freedom})=t$ value, p value, number of preparations.
- 260 • One way repeated measures ANOVA: $F(\text{degrees of freedom, residual})=f$ value, p value, posthoc
261 test, number of experiments.

262 "N" denotes the number of preparations, while "n" is the number of trials/APs. Significant differences are
263 indicated using * $p<0.05$, ** $p<0.01$, *** $p<0.001$. Exact p values are given unless they were smaller than
264 0.001, in which case $p<0.001$ is indicated. Post-hoc tests were carried out for a significance level of
265 $p<0.05$ unless otherwise stated. Type of experimental design: Random.

266 **RESULTS**

267 STG neurons are heavily modulated by descending projection neurons that release a variety of different
268 modulators, including neuropeptides and biogenic amines (summarized in Marder and Bucher, 2001;
269 Selverston et al., 2009; Stein, 2009; Blitz and Nusbaum, 2011). The axons of several neurons are
270 sensitive to biogenic amines in that focal application of these drugs to axonal regions elicits secondary,

State-dependent modification of sensory sensitivity via modulation of backpropagating action potentials

271 ectopic SIZs and backpropagating APs (Meyrand et al., 1992; Bucher et al., 2003; Goillard et al., 2004;
272 Städele and Stein, 2016). Despite this, there is no direct evidence that modulatory control of ectopic APs
273 is indeed employed by projection neurons and that such modulation affects the function of the modulated
274 neuron.

275 We studied whether the IV neurons, a pair of aminergic descending projection neurons, affect ectopic AP
276 production in the axon of the single-cell muscle tendon organ AGR, and how this modulation affects the
277 encoding of sensory stimuli. AGR and the IV neurons contribute to the same behavior in that they serve
278 complementary functions in feeding. In *C. borealis*, the IV neurons activate rhythmically when the animal
279 encounters food with its antennae (Hedrich and Stein, 2008), usually immediately before food is cleaved
280 by the mandibles and enters the stomach. Activation of the IV neurons causes a long-lasting gastric mill
281 rhythm in the stomach that drives three internal teeth in mastication within the lumen of the stomach.
282 Once the gastric mill rhythm is running, AGR senses muscle tension of the gm1 protractor muscles during
283 the powerstroke of the medial tooth and generates bursts of APs near its dendrites in the muscle. Its
284 feedback controls timing and strength of the gastric mill activity (Smarandache et al., 2008). Functionally,
285 thus, IV neuron activity precedes AGR activity, but both can continue throughout feeding. The IV neurons
286 project from the brain through the unilateral inferior ventricular nerve (*ivn*) and innervate the STG and the
287 CoGs (Fig. 1A). Importantly, they can be selectively activated by extracellular stimulation of the *ivn*
288 (Hedrich and Stein, 2008), which like chemosensory stimulation of the antennae elicits a gastric mill
289 rhythm.

290 Part of AGR's normal activity repertoire is the generation of APs at two different SIZs. Low frequency (3-9
291 Hz) ectopic APs are generated tonically in posterior parts of the *stn* (in the trunk of the central AGR axon)
292 (Daur et al., 2009; Städele and Stein, 2016). Higher frequency bursts of APs (15 - 40 Hz) are induced in
293 the peripheral anterior gastric nerve (*agn*), close to *gm1* muscles, and encode muscle tension (Combes et
294 al., 1995; Smarandache et al., 2008). Whenever muscle tension is low, ectopic APs are initiated at the
295 ectopic SIZ in the *stn*, and the peripheral SIZ is silent.

296 **AGR's ectopic spike activity is influenced by IV projection neurons**

297 To test whether the IV neurons modulate AGR's ectopic spiking, we stimulated the *ivn* and monitored
298 AGR's ectopic spike frequency extracellularly, along with several gastric mill motor neurons. Figure 1B
299 shows original recordings of AGR and the gastric mill neurons before and during consecutive *ivn*
300 stimulation with 40 Hz (10 trains, 6 sec train/intertrain duration). Stimulation parameters were selected
301 according to the published *in vivo* activity of the IV neurons (Hedrich and Stein, 2008). We observed a
302 strong decrease in AGR's ectopic firing frequency in response to IV stimulation, in this particular example
303 from 3.9 Hz to 2.3 Hz ($\Delta f = -1.6$ Hz). This diminishment outlasted the stimulation for more than 300
304 seconds.

305 As previously described (Christie et al., 2004; Hedrich and Stein, 2008), IV neuron stimulation elicited a
306 long-lasting gastric mill rhythm, apparent by the alternating burst activity of the lateral gastric (LG) and the
307 dorsal gastric (DG) neuron (Fig. 1B, bottom). Similar to previous observations (Goldsmith et al., 2014;
308 Städele and Stein, 2016) we found that the gastric mill rhythm was accompanied by small rhythmic
309 frequency changes in AGR (arrows in Fig. 1B) which are likely to be mediated by the gastric mill (GM)
310 motor neurons that are active in the same phase as LG. The decrease in AGR firing frequency could be
311 prolonged when IV neurons were stimulated for longer durations (up to 40 stimulus trains, N=5, data not
312 shown). In these cases, the beginning of the recovery back to baseline frequency was also delayed until
313 the end of the stimulation.

314 To characterize the IV neuron mediated effect, we measured AGR firing frequency before IV stimulation
315 (control), during the 5th and 10th stimulation train, and 80sec and 200sec after the last stimulation (Fig.
316 1C). On average (N=14), AGR firing frequency was significantly diminished starting with the 5th
317 stimulation and up to 200 sec after the end of IV stimulation, with the largest decrease at the 10th
318 stimulation (from 4.5 ± 1.3 Hz to 3.1 ± 1.1 Hz, $\Delta f = -1.3 \pm 0.3$ Hz, one way RM ANOVA, $F(13,4) = 49.21$,
319 $p < 0.001$, Holm-Sidak post-hoc test with $p < 0.05$). *In vivo*, the response of the IV neurons to chemosensory
320 stimuli at the antennae is quite variable (Hedrich and Stein, 2008), and ranges between 10 and 50 Hz,
321 probably due to the saliency of the chemosensory stimulus. We thus tested a variety of IV neuron
322 stimulus frequencies and found that the response of AGR to IV neuron stimulation depended on

323 stimulation frequency. When we stimulated the IV neurons with frequencies ranging from 10 to 50 Hz, in
324 10 Hz intervals (Fig. 1D), a significant diminishment in AGR firing frequency was observed at stimulation
325 frequencies of 20 Hz and above (One way RM ANOVA, $F(4,4)=49.21$, $p<0.001$, Holm-Sidak post-hoc test
326 with $p<0.01$ significance level, $N=10$). Thus, IV neuron firing frequency determined how strongly AGR
327 firing frequency was diminished, indicating that the strength of the chemosensory stimulus differentially
328 affects AGR ectopic spiking.

329 ***IV neurons alter AGR's axonal membrane excitability***

330 Only one of the two AGR SIZs is active at a given time. The current hypothesis is that the ectopic SIZ has
331 the higher intrinsic membrane excitability and thus dominates AGR's firing in the absence of sensory
332 spikes (Daur et al., 2009). However, when the excitability at the ectopic SIZ is artificially reduced, the
333 location of spike initiation switches, and the sensory SIZ in the *agn* starts spiking even in the absence of
334 muscle tension (Daur et al., 2009; Städele and Stein, 2016). In some of our experiments, we observed a
335 switch in spike initiation from the *stn* to the periphery during IV stimulation. In 9 of 45 experiments, the
336 decrease in AGR ectopic firing frequency was so dramatic that spike initiation switched from the *stn* to the
337 periphery. Figure 2A shows the switch in AGR spike initiation exemplarily for one preparation. In this
338 particular example, IV neuron activation initially diminished AGR firing frequency by about 25%, until a
339 steady state was reached. At that time, spike polarization of AGR on the *dgn* changed noticeably (arrows
340 in Fig. 2A'), indicating that the direction of AP propagation switched and APs were initiated elsewhere
341 (described by Daur et al., 2009; Städele and Stein, 2016). To determine where APs were initiated, we
342 compared the delay in spike appearance between multiple extracellular recording sites along the AGR
343 axon (peripheral: dorsal gastric nerve (*dgn*), central: stomatogastric nerve (*stn*), close to the CoGs:
344 superior esophageal nerve (*son*)). We found that spikes with negative deflection (blue, Fig 2A) always
345 occurred first on the *stn* recording site (Fig. 2B, i), and traveled orthodromically towards the *sons* and
346 antidromically towards the peripheral *dgn*. In contrast, spikes with positive deflection (green, Fig. 2A)
347 always occurred first on the *dgn* and propagated only orthodromically towards the *stn* and *sons* (Fig. 2B,
348 ii). Spike initiation switched back and forth between the ectopic and sensory SIZ, indicating that the
349 membrane excitability of the ectopic SIZs fell below that of the peripheral one. We noticed that during the

350 switches the temporal accuracy of APs was reduced in that APs arrived with slightly different delays
351 ('jitter') at the extracellular recording sites (Fig. 2ii, right). This may indicate that APs were either not
352 initiated at a fixed location or that propagation velocity varied. In four additional experiments, the
353 diminishing effect of the IV neurons turned off spike initiation completely (Fig. 2C). In conclusion, our
354 results so far predict that IV neurons alter spike initiation in the AGR axon most likely by reducing axonal
355 membrane excitability.

356 ***IV neurons control ectopic spiking via release of histamine***

357 The IV neurons exert their actions on the STG motor circuits directly via histaminergic inhibition of STG
358 circuits, and indirectly via activation of other modulatory projection neurons in the commissural ganglia
359 (Christie et al., 2004; Hedrich et al., 2009). Their latter actions are required for eliciting the gastric mill
360 rhythm and involve at least two identified CoG projection neurons (Christie et al., 2004; Hedrich et al.,
361 2009; Hedrich et al., 2011). Since the observed decrease in AGR firing frequency during IV neuron
362 stimulation was always accompanied by a gastric mill rhythm, we wanted to exclude that the decrease
363 was due to the involvement of CoG projection neurons. To test this, we elicited gastric mill rhythms that
364 involved the same two identified projection neurons known to mediate the IV neuron-induced gastric mill
365 rhythm. In this case, however, the rhythm was activated via stimulation of the mechanosensory ventral
366 cardiac neurons (VCN; Beenhakker et al., 2004). While the elicited gastric mill rhythm (Fig. 3A) was
367 accompanied by small rhythmic firing frequency changes in AGR during the activity phase of the GM
368 neurons (Goldsmith et al., 2014; Städele and Stein, 2016), VCN activation did not cause a significant
369 decrease in AGR firing frequency. This was true for all preparations tested (Fig. 3B) (one way RM
370 ANOVA, $F(11,4)=4.17$, $p=0.06$, $N=8$). With the exception of the small rhythmic firing frequency changes,
371 AGR firing frequency remained unaffected during and after VCN stimulation. This indicated that the
372 decrease in AGR firing frequency was specific to the IV neurons and not dependent on the activation of
373 CoG projection neurons.

374 To further scrutinize this result we completely removed both CoGs by transecting the *ions* and *sons*. This
375 kept the direct connection between IV neurons and STG intact but eliminated indirect effects via CoG
376 neurons. Figure 3C shows the decrease in AGR ectopic firing frequency in response to IV neuron

377 stimulation before and after CoG transection. Across preparations (Fig. 3D) the decrease in AGR firing
378 frequency did not significantly change when the CoGs were transected (comparison of AGR ff. after 5th
379 stim, one way RM ANOVA, $F(3,17)=32.36$, $p<0.001$, Holm-Sidak post-hoc test with $p<0.01$, $N=6$).
380 However, as expected, without CoGs IV neuron stimulation did not elicit a gastric mill rhythm, and the
381 small gastric mill-timed AGR rhythmic frequency changes were absent.

382 To test whether the decrease in AGR firing frequency during IV neuron stimulation could be chemically
383 transmitted, we blocked chemical transmission at AGR's ectopic SIZ by reducing the extracellular Ca^{2+}
384 concentration. Specifically, we focally applied low Ca^{2+} saline to the posterior part of the *stn* (close to the
385 STG neuropil edge). Low Ca^{2+} saline prevented the IV neuron-induced decrease in AGR firing frequency
386 in all experiments ($N=6$) (Fig. 3Ciii, 3D), suggesting that the IV neuron effect is mediated chemically.
387 Besides histamine, the IV neurons contain the co-transmitter FMRF-like peptide F1 (Christie et al., 2004).
388 Furthermore, Li and colleagues (2002) suggested that the IV neurons might also contain different
389 Orcokinin isoforms. To test whether any of the identified IV co-transmitters can mediate the observed
390 diminishment in AGR firing frequency, we bath applied them individually at different concentrations to the
391 posterior part of *stn*, where AGR's ectopic SIZ is located. Figures 4A and B show AGR's response to
392 modulator application. Measurements were taken in steady state, i.e. 5 minutes after application.
393 Application of 100 μ M FMRF-like peptide F1 to the posterior part of the *stn* excited AGR and elicited a
394 strong increase in firing frequency (Fig. 4A). This increase was concentration-dependent: 1 μ M FMRF-like
395 peptide already caused an increase in AGR firing frequency, but the effect was much smaller (data not
396 shown). On average we found that 100 μ M FMRF-like peptide caused a significant increase in AGR firing
397 frequency by $32\pm 15\%$ (paired t-test, $t(5)=-6.42$, $p=0.001$, $N=6$) (Fig. 4A'). In all cases, the time constant of
398 the increase was slow and steady state was reached after about 120 sec. Application of histamine
399 (10mM), in contrast, caused a strong diminishment in AGR firing frequency (Fig. 4B) with a similar time
400 course as seen during IV neuron activation. On average, histamine caused a significant decrease in AGR
401 firing frequency by $28\pm 9\%$ (paired t-test, $t(12)=6.18$, $p=0.001$, $N=13$) (Fig. 4B') that outlasted the
402 application by about 250 sec. In five out of 13 experiments, the decrease in AGR firing frequency was
403 strong enough to switch the site of ectopic spike initiation to the *dgn* (arrows in Fig. 4B). In none of our
404 experiments ($N=5$) did application of any of the two Orcokinin isoforms tested ($[Ala^{13}]$ and $[Val^{13}]$, 1 to 100

405 μM (Li et al., 2002)) elicit a change in AGR firing frequency, despite the fact that both isoforms influenced
406 the pyloric and gastric mill rhythms when applied to the STG (data not shown).

407 To validate that release of histamine from the IV neurons caused the diminishment of AGR's firing
408 frequency, we used cimetidine to block histaminergic actions during IV neuron stimulation. Cimetidine is
409 an H_2 receptor antagonist known to diminish IV neuron-mediated histaminergic effects in the STG
410 (Christie et al., 2004). Specifically, we stimulated the IV neurons in regular saline, observed the decrease
411 in AGR firing frequency, applied cimetidine (5 mM) to AGR's ectopic SIZ in the posterior *stn*, and then
412 stimulated the IV neurons again. Figure 4C shows the response of AGR to IV neuron stimulation before
413 and during cimetidine application. AGR's decrease was strongly reduced in cimetidine (trace ii), indicating
414 that histamine release contributed to the IV neurons' effect on AGR. Across preparations (Fig. 4D), we
415 found that in the presence of cimetidine IV neuron stimulation no longer diminished AGR's firing
416 frequency (paired t-test, $t(4)=2.66$, $p=0.056$, $N=5$). In summary, thus, our results demonstrate that
417 histamine released from the IV neurons diminished AGR firing frequency, likely via H_2 receptor activation.

418 ***IV neuron modulation of the AGR axon is spatially restricted***

419 If the IV neuron-elicited decrease in AGR firing frequency is specific to ectopic APs and their initiation site
420 in the axon, it should not affect APs generated in the sensory dendrites. To test this, we artificially moved
421 the site of spike initiation away from the posterior part of the *stn* to the *dgn* via focal application of high-
422 divalent saline (HiDi) to the *stn*. HiDi diminishes membrane excitability, thereby inactivating AGR's ectopic
423 SIZ and allowing the peripheral SIZ to become active (Daur et al., 2009; Stadele and Stein, 2016).
424 Figures 5A and B show an example of this switch in SIZs. We then activated the IV neurons to test
425 whether AGR firing frequency is still diminished when APs are initiated in the peripheral dendrites. Similar
426 to the control experiments in regular saline, IV neuron stimulation in HiDi elicited a strong and long-lasting
427 gastric mill rhythm, indicating that the stimulation was successful. Yet, with the peripheral SIZ active, AGR
428 firing frequency did not decrease anymore (Fig. 5B'). We found this to be true for all preparations tested
429 (average change in AGR ff. in comparison to baseline: Δf control= 1.68 ± 0.58 Hz, Δf HiDi= 0.02 ± 0.06 Hz,
430 $N=5$). We also observed that the small gastric mill-timed oscillations of the AGR firing frequency were
431 absent when APs were initiated in the peripheral dendrites. In conclusion, descending IV neuron

432 modulation specifically targeted the ectopic SIZ in the *stn*, allowing a direct regulation of ectopic spike
433 frequency at this site.

434 ***IV neurons modify sensory encoding in AGR***

435 Ectopic APs travel both ortho- and antidromically. While it has been shown that orthodromic APs add to
436 already existing APs and increase a neuron's spike frequency, the influence of antidromic APs is less
437 clear. Unless collisions with existing APs occur, antidromic APs may propagate into dendritic regions with
438 the potential to affect information encoding (Dubuc et al., 1988; Beloozerova and Rossignol, 2004; Ma
439 and LaMotte, 2007). Synaptic processing in neocortex and hippocampus, for example, is altered by APs
440 initiated at the axon initial segment that backpropagate into dendritic areas and modify subsequent signal
441 encoding (Markram et al., 1997; Wu et al., 2012; Bukalo et al., 2013). Similarly, in chordotonal organs of
442 the crayfish leg, back-propagating APs can change the sensitivity of sensory neurons to leg movements.
443 In our experiments, we have so far found that the chemosensory IV neurons modulate the spontaneous
444 ectopic APs in AGR without fully abolishing ectopic spiking. We thus hypothesized that changes in
445 ectopic frequency (and not just their presence or absence) will alter AGR's sensory activity. We reasoned
446 that ectopic APs invade the sensory dendrites, where they affect membrane excitability and hence AGR's
447 sensory burst properties. To test this, we induced sensory bursts in AGR, and then compared the elicited
448 bursts at a range of AGR ectopic spike frequencies. To reduce experimental variability in spontaneous
449 and IV neuron-induced ectopic firing frequencies between animals, we induced ectopic APs via
450 extracellular stimulation of the posterior part of the *stn*. Hereinafter, we use the term siAP to distinguish
451 stimulation-induced ectopic APs from spontaneous APs. We elicited siAPs at frequencies between 3 and
452 10 Hz, which is the range of ectopic spike frequencies observed *in vivo* (Daur et al., 2009; Daur et al.,
453 2012; DeMaegd and Stein, 2018). To avoid interference of siAPs and spontaneously induced APs we did
454 not decrease the stimulation frequency below 3Hz.

455 We induced sensory bursts in AGR in a semi-intact preparation in which the gm1 muscles were kept
456 intact, but the rest of the nervous system was dissected as in the previous experiments. The muscles
457 were pinned down at the anterior ossicles while the posterior ossicles were attached to a stimulus clamp
458 controlled by an electrical manipulator. We then stretched the muscle to increase muscle tension by

459 pulling the posterior ossicles (see Materials and Methods; Smarandache and Stein, 2007). siAP
460 frequencies were applied in random order to prevent time or hysteresis effects, and each frequency was
461 repeated two times at random intervals. Each siAP frequency trial was preceded by a control muscle
462 stretch with no siAP stimulation, and followed by another control stretch. Muscle stretch was followed by a
463 waiting period of two minutes to minimize potential history-dependent influences of past bursts. This
464 ensured that for each muscle stretch, AGR was in a fully recovered state, i.e. sufficiently rested so that its
465 response was independent of previous stimuli or stretches. As a consequence, however, experiments
466 required the muscles to be healthy for several hours. To minimize muscle fatigue the holding phase of the
467 muscle stretch was kept short (0.5s). Across animals, the average and maximum frequencies of the
468 elicited bursts ranged from 11 Hz to 25 Hz (average intraburst firing frequency) and 21 Hz to 37 Hz
469 (maximum firing frequency in the burst) and were thus within the extent observed in previous *in vivo*
470 recordings of AGR (Smarandache et al., 2008). Figure 6A shows an example recording of AGR's sensory
471 burst on the *stn* following a siAP frequency decrease from 7 to 3 Hz. In this particular preparation, the
472 decrease in siAP frequency caused a prolongation of the sensory burst by 0.78 sec (from 0.53 to 1.31
473 sec). As expected, siAPs first occurred on the *stn* and traveled bidirectionally towards the *son*
474 (orthodromic) and the *dgn* (antidromic) (Fig. 6B, top). However, during the sensory burst, APs were
475 elicited in the periphery and only traveled orthodromically from the *dgn* towards the *stn* and *son* (Fig. 6B,
476 middle). After the end of the sensory burst, AGR regained spontaneous ectopic spike activity. Like the
477 siAPs, these spontaneous APs were initiated on the *stn* and traveled bidirectionally towards the *son* and
478 *dgn* (Fig. 6B, bottom).

479 Despite our preventative measures, we still observed muscle fatigue and substantial reduction in sensory
480 response over time due to the duration of the experiment. While this could be partially compensated by
481 increasing muscle stretch, it affected baseline sensory responses in AGR. To assess the influence of
482 siAPs on AGR's response, we thus calculated relative changes (in percent) elicited by the siAP
483 stimulation with respect to the two control muscle stretches immediately before and after siAP stimulation.
484 Across preparations (N=8), we found that diminishing siAP frequency significantly reduced the change in
485 burst duration from the control burst, signifying prolongation of burst duration with decreasing siAP
486 frequency (Fig. 6C, one way RM ANOVA, $F(7,42)=3.831$, $p=0.003$, $N=8$). Posthoc comparison revealed

487 that bursts were significantly prolonged with siAP frequency decreases of 5 Hz or more (Student-
488 Newman-Keuls posthoc test, $p < 0.05$, $N=8$). The number of spikes per burst also followed a similar trend,
489 in which diminishing siAP frequency significantly reduced the difference in the number of spikes per burst
490 from the control burst, signifying an increase in the number of spikes per burst (Fig. 6D, one way RM
491 ANOVA, $F(7,42)=9.717$, $p < 0.001$, $N=8$). Spike number decreased continuously from 10 Hz to 3 Hz siAP
492 frequency. Posthoc pairwise comparison revealed significant increases in the number of spikes per burst
493 with decreases of siAP frequency of 3 Hz or more (Student-Newman-Keuls posthoc test, $p < 0.05$, $N=8$).
494 By contrast, there was no significant trend for the average intraburst spike frequency (Fig. 6E, one way
495 RM ANOVA $F(9,56)=1.198$, $p=0.315$, $N=8$). This was likely due to burst duration and spike number
496 changing equally.

497 Because we kept muscle stretches short to prevent muscle fatigue, we were unable to account for the
498 effects of ectopic AP frequencies on longer AGR bursts. We thus employed a second approach for
499 initiating sensory bursts. In this case, we focally applied high K^+ saline to the AGR's peripheral dendrites
500 Figure 7A shows an example recording of AGR's sensory burst on the *stn* following a siAP frequency
501 decrease from 7 to 3 Hz. In this particular preparation, the decrease in siAP frequency caused a
502 prolongation of the K^+ induced sensory burst by 2.9 sec (from 3.3 to 6.2 sec). Similar to the semi-intact
503 preparation, siAPs traveled bidirectionally towards the *son* (orthodromic) and the *dgn* (antidromic) (Fig.
504 7B, top), and sensory APs only traveled orthodromically from the *dgn* towards the *stn* and *son* (Fig. 7B,
505 middle). Spontaneous APs after the sensory burst were again initiated on the *stn* and traveled
506 bidirectionally on the AGR axon (Fig. 7B, bottom). We did not observe substantial reductions in sensory
507 responses over time in these experiments, allowing us to assess AGR responses without further
508 normalization. Across preparations ($N=5$), we found a significant prolongation of burst duration with
509 decreasing siAP frequency (Fig. 7C, one way RM ANOVA, $F(4,28)=4.65$, $p=0.001$). Specifically, K^+
510 application elicited the shortest bursts when AGR was pre-activated with 10 to 6 Hz siAP frequency (no
511 significant difference between 10-6 Hz). From then on, burst duration steadily increased with smaller siAP
512 frequencies until the siAP frequency reached 3 Hz. Burst prolongation was significant for decreases of 2
513 Hz or more (Δ duration from 3-7 Hz= 2.6 ± 2.3 sec, 6-3 Hz= 2.5 ± 2.2 sec, 5-3 Hz= 2.0 ± 2.1 sec; Student-
514 Newman-Keuls posthoc test, $p < 0.05$, $N=5$). The duration of sensory-induced bursts was thus most

515 strongly affected when the ectopic firing frequency of AGR decreased from 5 Hz (and above) to 3 Hz,
516 which matches the physiological frequency decrease elicited by IV stimulation.

517 In addition, the number of spikes per burst increased significantly when siAP frequency was reduced from
518 7 to 3 Hz (Fig. 7D, one way RM ANOVA, $F(4,28)=3.29$, $p=0.038$, Student-Newman-Keuls posthoc test,
519 $p<0.05$, $N=5$). Similar to the muscle stretch experiments, the average intraburst spike frequency remained
520 unchanged (Fig. 7E, one way RM ANOVA, $F(4,28)=1.07$, $p=0.15$, $N=5$). In conclusion, these data indicate
521 that ectopic APs that penetrate sensory dendrites are capable of altering the duration and spike number
522 of sensory bursts and thus sensory encoding.

523 ***A slow K^+ current is sufficient to modify sensory bursts***

524 Which properties of the peripheral dendrites allowed ectopic APs to affect the sensory burst? APs that
525 invade stimulus-encoding dendrites can strengthen synaptic input through the accumulation of ions or
526 ionic currents over time (Markram et al., 1997; Wu et al., 2012), or require specific ion channels that affect
527 postsynaptic responses, such as L-type Calcium channels (Bukalo et al., 2013). For neurons that
528 transduce sensory stimuli instead of receiving synaptic input, it is unclear what intrinsic properties might
529 facilitate the modulatory effect backpropagating APs have on sensory responses (Bevengut et al., 1997).
530 Since in AGR the sensory burst was shorter with higher ectopic AP frequencies, we hypothesized that
531 slowly accumulating hyperpolarizing currents may exist in the peripheral dendrites that facilitate this
532 effect. Previous model data had indeed suggested that AGR contains a slow Ca^{2+} -activated potassium
533 current (Daur et al., 2012). To address whether a slow hyperpolarizing current is sufficient to enable
534 sensory modulation by ectopic APs, we created a computational model axon using *MadSim* (Daur et al.,
535 2012; Städele et al., 2015). Briefly, we used a single compartment with active properties connected to
536 three passive dendritic compartments to model the peripheral SIZ and the sensory dendrites,
537 respectively. The neuron had a resting potential of -60 mV (similar to AGR, Daur et al., 2012), and thus
538 showed no spontaneous activity. Similar to our physiology experiments, we elicited tonic APs with 7 to 3
539 Hz (1 Hz step intervals) with pulsed current injections. These stimulation induced APs represented AGR's
540 ectopic firing. Sensory bursts were mimicked with ramp-and-hold current stimuli. At least 20 siAPs were
541 elicited before the burst was initiated, and siAPs stopped upon burst start. We initially added a slow K^+

542 current (I_{KS}) with a time constant of activation (τ) of 2 sec. We reasoned that to have any effect, the
543 current must accumulate over time, and thus the time constant must be close to the interspike interval of
544 the siAPs. Figure 8A shows the change in burst duration of these models for different siAP frequencies.
545 With decreasing siAP frequencies burst onsets occurred prematurely and burst durations were prolonged.
546 This was consistent with our experimental findings in that lower ectopic AP frequencies caused bursts of
547 longer duration.

548 To test whether I_{KS} was indeed responsible for this observation, we removed it completely from the model,
549 leaving us with a simple Hodgkin and Huxley type neuron (Agüera y Arcas et al., 2003), in which the fast
550 Sodium and Potassium currents were the only voltage-gated currents. Without I_{KS} , bursts in these models
551 were mostly unaffected by the presence of the siAPs (Figs. 8B-D), and neither burst duration nor the
552 number of spikes per burst showed a strong dependence on siAP frequency. Thus, these data indicate
553 that a slow potassium current is sufficient to elicit the frequency-dependent modulation of the sensory
554 burst by ectopic APs.

555 Next, we tested whether having a slow time constant is sufficient to achieve the observed effect. We thus
556 implemented different time constants for I_{KS} activation ($\tau = 0.25, 0.5, 1, 2,$ and 4 sec). A clear frequency-
557 dependent effect similar to our physiology experiments was only achieved with I_{KS} time constants of 1 sec
558 and longer (Fig. 8B). With a time constant of 0.25 sec, the effect was even opposite to what we had
559 observed in our experiments: decreasing siAP frequencies caused shorter bursts with fewer spikes per
560 bursts (red trace in Fig. 8C). In addition, the average intraburst firing frequency (Fig. 8D) was slightly
561 increased, although no frequency-dependent change was obvious. In contrast, with time constants of 1
562 and 2 sec, reducing siAP frequency prolonged the burst, elicited more spikes per burst, and did not alter
563 intraburst firing frequencies. A time constant of 4 sec, however, had no further effect on burst duration,
564 but increased the frequency-dependent influence on the number of spikes per burst and caused a slight
565 reduction in intraburst firing frequency.

566 Taken together, our data suggest that a slowly accumulating K^+ current is sufficient to elicit the observed
567 changes in the sensory bursts. Furthermore, the strength and frequency-dependence of these changes
568 seem to be determined by the time constant of activation, i.e. how fast the I_{KS} accumulated. We used siAP

569 frequencies between 3 Hz and 7 Hz, and thus interspike intervals between 333 and 143 ms. However,
570 only I_{KS} time constants of 1 sec and more caused the expected frequency-dependent effect. The model
571 thus predicts that the time constant of the current must be at least several fold larger than the ectopic
572 interspike interval. Modification of stimulus encoding via antidromic APs penetrating peripheral dendrites
573 may therefore represent a general phenomenon in neurons that have slow currents similar to I_{KS} .

574 ***IV neurons do not affect AP propagation fidelity along the AGR axon***

575 Numerous studies have reported activity-dependent changes in axonal conduction velocities (reviewed by
576 Bucher and Goaillard, 2011). In the presence of neuromodulators, propagation dynamics can further
577 change, resulting in modified interspike intervals. This alters AP frequencies as they propagate from the
578 site of spike initiation to the axon terminal, potentially changing transmitter release onto postsynaptic
579 neurons (Lang et al., 2006; Ballo and Bucher, 2009). Since AGR's sensory APs must travel through the
580 area where the IV neurons diminish axonal membrane excitability, we tested whether the observed
581 decrease in sensory burst duration indeed is faithfully conducted onto postsynaptic neurons during IV
582 induced axonal neuromodulation. Specifically, we first tested whether axonal conducting velocity of en-
583 passant APs was affected by IV activation as they pass the site of modulation. For this, we activated AGR
584 in the periphery and measured the delays at which APs arrived near the CoG, before and during IV
585 stimulation. AGR was stimulated extracellularly on the *agn* with 5 consecutive trains, each with 28 pulse
586 and 15 Hz stimulation frequency. This approximates AGR's mean sensory burst frequency *in vivo* (Daur
587 et al., 2009; Daur et al., 2012) and during K^+ application to the *dgn*. At this frequency, peripheral
588 stimulation overrides all ectopic APs, allowing us to test modulatory effects on the axon without the
589 interference of ectopic APs. Figure 9A shows an example of the temporal occurrence of APs on the *dgn*
590 and the *son* in one experiment. APs were aligned to the corresponding stimulus and plotted on top of
591 each other so that the first spike appears at the bottom and the last one at the top. We found that the
592 AGR conduction velocity was history-dependent even in the absence of IV activation in that it initially
593 decreased and then increased (blue lines in Fig.9A). For analysis, we plotted resulting AP arrival times as
594 a function of spike number. Figure 9B shows that for this particular experiment the pattern of temporal AP
595 appearance during IV neuron stimulation did not change when compared to control condition. This was
596 consistent for all preparations tested (Fig. 9C). On average, there was no significant change in AP

State-dependent modification of sensory sensitivity via modulation of backpropagating action potentials

597 propagation dynamics during IV stimulation when compared to the no-stimulus control (one sided paired
598 t-test, $t(27) = -0.89$, $p = 0.38$, $N = 6$). To conclude, IV neuron modulation of the AGR axon did not influence
599 the temporal dynamics of en-passant APs.

600 However, our experiments were only designed to test for immediate effects IV neurons might exert on AP
601 conduction velocity (~50-100 sec after the onset of IV stimulation). Long-lasting neuronal activity has
602 been shown to further modulate axonal excitability and thus AP propagation dynamics (Zhang et al.,
603 2017). The IV neuron effect on these slow mechanisms were not tested in our experiments.

604 Moderate or high frequency stimulation (10-50 Hz) of axons can lead to propagation failures (Krnjevic and
605 Miledi, 1959; Grossman et al., 1979) so that information is 'deleted' along the axon before being
606 conveyed onto postsynaptic partners. Excitability changes in the axon can dramatically affect the rate of
607 conduction failures (Debanne, 2004), and thus change the computational capability of the axon (its
608 'fidelity'). Since the IV neurons diminished the AGR axon excitability, we speculated that the rate of
609 propagation failures and the maximum transmission frequency at which the AGR axon is able to conduct
610 APs is diminished by IV neuron modulation. To test this, we stimulated the *agn* with 10 consecutive trains
611 of 10 to 50 Hz (10 Hz steps) for 9 seconds and compared the number of spikes passing through the site
612 of modulation before and during IV neuron activation. 50 Hz stimulation reliably caused spike failures of
613 >50% (2385 ± 585 pulses out of 4500, $N = 8$) even in the absence of IV neuron activation, indicating that
614 reliable AP propagation in AGR is limited to lower frequencies. Stimulation frequencies between 10 and
615 30 Hz reliably elicited APs without any spike failures in control and during IV activation. Yet, at 40 Hz
616 spike failures started to occur both in control and during IV neuron stimulation. Figure 9D shows an
617 example of AGR's responses to 40 Hz *agn* stimulation before and during IV neuron activation. However,
618 we found no significant difference between the number of spike failing during IV neuron modulation and
619 the no-stimulation control (Fig. 9E) (control: 64 ± 68 failures, during IV stim: 62 ± 62 failures, paired t-test,
620 $t(7) = 0.7$, $p = 0.5$, $N = 8$). Taken together, our results demonstrate that descending modulation of the AGR
621 axon by IV neurons affected neither maximum transmission frequency nor axonal propagation fidelity.

622 **DISCUSSION**

623 The sensitivity of many sensory neurons are state- and context-dependent. Consequently, sensory
624 activity does not solely depend on stimulus properties, but also on internal and external conditions of the
625 animal. Backpropagation of action potentials into the stimulus encoding sites of neurons has been
626 implicated in altering synaptic and sensory stimulus encoding, but to our knowledge, this is the first study
627 to demonstrate that backpropagating ectopic APs dynamically modify sensory encoding in response to
628 modulation by descending projection neurons.

629 ***Neuromodulation of sensory systems.***

630 The ability of the neuromodulatory system to globally affect sensory systems has long been established
631 (Birmingham, 2001). The intensity of reflexes such as startle responses, for example, are altered by
632 monoamines, peptides, and opiates (Davis, 1980). Sensory modulation is not limited to reflexes, however,
633 and can affect aspects of social communication (Hoke and Pitts, 2012), taste (Lemon, 2017), olfaction
634 (Kawai et al., 1999), hearing (Brozoski and Bauer, 2016), and pain (Tsuda, 2017). While initially thought
635 to allow the animal to optimize energy expenditure, it is now clear that modulating sensory responses is a
636 common phenomenon that allows organisms to dynamically modify sensory responses in a variety of
637 external and internal conditions.

638 Contrary to endocrine and paracrine actions, direct and more local control of sensory sensitivity by the
639 CNS is not well understood, with the exception of sensory gating via presynaptic inhibition that leads to a
640 diminishment or even complete block of afferent spike propagation into sensory terminals (El Manira and
641 Clarac, 1994; Coleman et al., 1995; Sauer et al., 1997; Stein and Schmitz, 1999; Beenhakker et al., 2005;
642 Beenhakker et al., 2007; Barriere et al., 2008; DeLong et al., 2009; Bardoni et al., 2013). Our results
643 show that while axonal membrane excitability in a sensory neuron, AGR, was diminished by histaminergic
644 actions of descending projection neurons, afferent spike propagation in AGR remained unaffected (Fig.
645 9). Specifically, neither AP propagation velocity, history-dependence, nor AP failure rate was altered. This
646 occurred despite the fact that global aminergic modulation has been shown to significantly alter AP
647 propagation dynamics in other axons of the same system (Panzeri et al., 2001; Ballo and Bucher, 2009;
648 Ballo et al., 2010; Ballo et al., 2012). However, these modulatory influences occur when large stretches of

649 the axon are exposed to modulation (Ballo and Bucher, 2009), which not the case for modulation by the
650 IV neurons. Instead, modulation appeared to be restricted to the location of the ectopic spike initiation
651 zone itself (Fig. 5), suggesting a different function of modulation besides influencing propagation of
652 sensory information.

653 Our main result is that descending projection neurons modulate the frequency of backpropagating APs,
654 and that this change in frequency modifies sensory sensitivity. There are many examples in which
655 additional APs are elicited in ectopic locations, i.e. spatially distant from the canonical spike initiation site
656 that supports the main function of the neuron. In STG motor neurons, dopamine can elicit additional APs
657 in the axon trunk (Bucher et al., 2003), in thalamocortical neurons, nicotinic modulation of axon terminals
658 in elicits additional APs (Lambe et al., 2003), and clinically therapeutic techniques such as Spinal Cord
659 Stimulation (SCS) or Deep Brain Stimulation (DBS) stimulate ectopic APs to alleviate symptoms of
660 neuropathic pain (Li et al., 2006) and Parkinson's disease (Garcia et al., 2005), respectively. These
661 ectopically generated APs add to already present orthodromic action potentials and correspondingly alter
662 synaptic output. Similar effects on postsynaptic neurons have been described for sensory neurons as well
663 (Städle and Stein, 2016). However, if ectopic APs are generated at the axon trunk or the axon terminal,
664 they also backpropagate antidromically towards the axon origin, reversing the functional polarization of
665 the neuron by carrying information about distant modulator actions to sites of stimulus encoding where
666 they can affect future encoding events. Previous studies on crayfish chordotonal organs have
667 demonstrated that backpropagating APs indeed can alter the sensitivity of velocity and position-
668 dependent sensory neurons that are involved in leg posture control (Bevengut et al., 1997). The sensory
669 axon terminals are excited by GABA-ergic primary afferent depolarizations that occur in phase with the
670 central pattern generator that drives leg movements. When suprathreshold, antidromic APs are elicited
671 that have the ability to alter the sensitivity to sensory stimuli (Bevengut et al., 1997). In this case, the
672 range of ectopic spike frequencies, origin of modulation and control of antidromic firing are unclear, as are
673 the mechanisms by which antidromic APs alter sensory sensitivity when they invade the sensory
674 dendrites. Underlying channels have been explored in CA1 hippocampal neurons, where antidromic APs
675 elicited by GABA_A-mediated depolarization and an additional electrotonic coupling at axon terminals

State-dependent modification of sensory sensitivity via modulation of backpropagating action potentials

676 cause long-lasting synaptic depression of incoming synaptic signals, resulting in a rescaling of synaptic
677 weights that may contribute to memory consolidation. Here, L-type Calcium channels are a prerequisite
678 for invading APs to have an effect on synaptic integration (Bukalo et al., 2013). While there are no
679 synaptic inputs in sensory dendrites, our models indicated that similarly to the CA1 neurons, passive
680 properties and Hodgkin-Huxley-type Sodium and Potassium currents are not sufficient to elicit such a
681 response, but a slowly accumulating ionic conductance was necessary. Specifically, our results show that
682 changes in IV neuron firing rate reduce AGR's ectopic spiking accordingly, and that this causes a
683 frequency-dependent increase in AGR's response. A slow hyperpolarizing current was sufficient to elicit
684 this effect in the model. It is reasonable to assume that a slow accumulation of outward currents will
685 hyperpolarize the dendrites, and reduce local excitability to sensory inputs. Interestingly, though, the time
686 constant of the current determined the sign of the response in that a fast time constant reversed the
687 frequency dependence, causing a diminished response with lower ectopic AP frequency. This indicates
688 that the rates of gate opening and closing determine whether there are frequency-dependent effects, and
689 if so, which direction they have. The different rates at which similar ion channels operate in different
690 neurons, even within the same organisms, is quite striking. It is conceivable, thus, that those rates are
691 adjusted to serve specific function for given neurons, and in case of backpropagating APs, to allow and
692 regulate effects on stimulus encoding. It is obvious that backpropagating APs may only exert effects if
693 they truly invade the dendritic structures though. This may not always be the case, as antidromic APs in
694 STG motor neurons have little effect on motor pattern generation (Bucher et al., 2003), and neurons may
695 be able to differentiate between orthodromically and antidromically propagating APs (Dugladze et al.,
696 2012).

697 Axon modulation and mechanisms

698 The actions and functions of neuromodulators on axons remain somewhat enigmatic, despite the fact that
699 membranes of myelinated and unmyelinated axon trunks are endowed with ionotropic and metabotropic
700 receptors for transmitters and neuromodulators (summarized by Bucher and Goillard, 2011; Sasaki et
701 al., 2011). We demonstrate that the IV neurons directly modulate the AGR axon and enable a frequency-
702 dependent change of sensory sensitivity in AGR. Like many other descending projection neurons

703 (Nusbaum, 2013), the IV neurons contain several co-transmitters (Christie et al., 2004; Stein et al., 2007).
704 Two of the IV neuron's co-transmitters, histamine and FMRF-like peptide, had the ability to alter AGR's
705 ectopic spike frequency in opposing ways. When applied to AGR's ectopic SIZ, histamine reduced AGR's
706 firing frequency similar as seen during IV neuron activation, while FMRF-like peptide increased the
707 ectopic firing frequency (Fig. 4). While the AGR axon is responsive to both transmitters, our results
708 indicate that only histamine is neuronally released at AGR's ectopic SIZ. When histamine actions were
709 blocked, we found no evidence of excitatory actions by the IV neurons on AGR's firing frequency,
710 indicating that FMRF-like peptide was not released at the *str*. This is consistent with the observation that
711 IV neuron transmitter actions seem to diverge in that they act on different neuronal structures. It has
712 previously been shown that most, if not all, direct actions of the IV neurons on the STG motor circuits are
713 mediated by histamine, while FMRF-like peptide actions were absent (Christie et al., 2004). On the other
714 hand, IV neuron actions on CoG neurons seem to be exclusively mediated by FMRF-like peptide.

715 Histamine, just like other biogenic amines, mediates a plethora of different actions on neurons
716 (summarized in Haas et al., 2008). It either acts through metabotropic G-protein coupled receptors (H_1 -
717 H_4) that mediate an increase in intracellular cAMP, or via ionotropic receptors that activate chloride
718 conductances (Hatton and Yang, 2001, Lee et al., 2004, Cebada and Garcia, 2007). In the stomatogastric
719 nervous system all hitherto described histaminergic actions are direct in that histamine elicits a fast and
720 strong hyperpolarization of pyloric pacemaker neurons in the STG (Claiborne and Selverston, 1984;
721 Pulver et al., 2003; Christie et al., 2004). In our experiments, histaminergic effects on AGR lasted for up
722 to 300 seconds, indicating that the kinetics are distinct from histaminergic actions on STG motor neurons.

723 What mechanisms could be responsible for the observed decrease in ectopic spike initiation during IV
724 neuron activity? Potential mechanisms include a reduction in depolarizing ionic conductances or
725 activation of hyperpolarizing conductances (e.g. chloride or potassium) and associated shunting by
726 histamine. We found that blocking H_2 receptors substantially diminished the IV neuron-mediated effect. H_2
727 receptors have been shown to interact with ionic conductance such as $I_{K(Ca)}$ (Haas and Konnerth, 1983;
728 Pedarzani and Storm, 1993) and I_H (McCormick and Williamson, 1991; Pedarzani and Storm, 1995).
729 While I_H is present in AGR (Daur et al., 2012), $I_{K(Ca)}$ has not been experimentally verified. A histamine-
730 induced decrease of I_H or an increase of $I_{K(Ca)}$, or a corresponding shift in their voltage- or calcium-

731 dependence, could alter cell resting potential, input resistance, and consequently spike activity. For
732 example, Ballo and colleagues (2010) show that axonal I_H depolarizes the resting membrane potential in
733 the axon and causes ectopic spike initiation. However, due to its depolarizing effect, I_H also affects AP
734 propagation. In specific, the strength of I_H influences the slow after-hyperpolarization (sAHP) of APs
735 during repetitive activity (Grafe et al., 1997; Soleng et al., 2003; Baginskas et al., 2009). The sAHP, in
736 turn, has been implicated in a general slowing of AP propagation (Bostock and Grafe, 1985; Moalem-
737 Taylor et al., 2007; Ballo et al., 2010; Ballo et al., 2012). The fact that in our experiments AP propagation
738 during IV neuron modulation did not change (Fig. 9) indicates that if H_2 receptors modulate I_H or another
739 conductance in AGR, this effect must be spatially restricted to the ectopic SIZ.

740 **Functional implications**

741 The stomatogastric nervous system is an extension of the CNS and controls aspects of feeding (Stein,
742 2017) that are mediated by striated muscles in the foregut. AGR and IV neuron function are closely
743 intertwined as they both pertain to the gastric mill rhythm, which controls the movement of three internal
744 teeth that masticate food in the stomach. The IV neurons respond to chemosensory stimulation of the
745 antennae, when food touches the mouth or is in close vicinity to it. This is the case immediately before
746 food is swallowed and enters the stomach, and starts the gastric mill rhythm (Böhm et al., 2001; Hedrich
747 and Stein, 2008). In contrast, AGR provides feedback about ongoing gastric mill rhythms, i.e. when food
748 has already entered the stomach and is being chewed. AGR responds to muscle tension in the large gm1
749 muscles that carry out the power stroke of the median tooth, and like its mammalian tendon-organ
750 counterparts, reinforces muscle force when resistance to a movement is encountered. Thus, IV neurons
751 and AGR complement each other; IV neurons precede AGR activity at the beginning of feeding, and AGR
752 entraining the rhythm once it is running. Our results show a direct interaction between these two
753 independent sensory pathways. We tested this using semi-intact and isolated nervous system preparation
754 in which the sensory neuron was fully functional, all spike frequencies operated within the previously
755 measured *in vivo* activities, and in which stimulation protocols were exclusively based on measured *in*
756 *vivo* activity. The IV neurons directly diminish ectopic spiking in AGR, which ultimately leads to an
757 increased sensitivity to muscle tension. AGR's response is maintained for longer and the number of APs
758 increases. This happens once the IV neurons are activated by food stimuli, before the gastric mill rhythm

State-dependent modification of sensory sensitivity via modulation of backpropagating action potentials

759 is started. Chemosensory stimuli thus prime the proprioceptive response of AGR in that its sensitivity to
760 resistance to tooth movements is heightened. Functionally, this may prepare the sensory system in the
761 stomach for incoming food and allow it to adequately and quickly respond to filling of the stomach, and
762 provide the appropriate strength necessary to carry out the chewing movements. Conversely, once all
763 food is ingested, the IV neuron activity is likely to subside, indicating that no further increase in tension
764 may occur, removing the need for AGR to possess heightened sensitivity. Interestingly, the IV neuron
765 response to chemosensory stimuli seem quite variable (Hedrich and Stein, 2008). Our results indicate
766 that this will translate into variable modulation of AGR's ectopic frequency and that proprioceptive
767 sensitivity will change along with it. The idea that antidromically traveling ectopic APs are under
768 modulatory control by other sensory pathways and alter sensory encoding is a particularly intriguing
769 concept, since it allows these structures to be primed for incoming sensory information detected earlier by
770 other sensory pathways.

771 Given that descending modulatory projection neurons are a hallmark of most sensorimotor systems
772 (Nusbaum, 2013), neuromodulation of sensory axons may be common to many systems and enable
773 state-dependent changes in sensory encoding or transmission.

774 The ability of backpropagating APs to alter signal encoding has been demonstrated in the neocortex and
775 hippocampus: APs can backpropagate from the axon initial segment into nearby dendritic areas, resulting
776 in modified signal encoding of subsequent inputs (Markram et al., 1997; Wu et al., 2012). In human C-
777 fibers, APs elicited at the axon initial segment can antidromically invade spatially separated dendrites and
778 reset these dendritic regions. This ensures that only one of the many sensory dendrites dominates the
779 sensory response (called a flip-flop), namely the one with the fastest and highest response to sensory
780 input. While this process seems to be specific to convergence of sensory information within neurons with
781 large and spatially distinct dendritic trees (see also AGR in lobster; Combes et al., 1993), it also indicates
782 that simply by invading areas where sensory stimuli are encoded, APs can alter sensory responses. The
783 implications of antidromic ectopic APs for stimulus encoding should be distinct from backpropagating APs
784 originating from the axon initial segment though. Since APs initiated at the axon initial segment are

785 always elicited after dendritic stimulus integration, backpropagation can only affect future stimulus
786 encoding. In contrast, our results demonstrate that a direct modulation of remotely initiated,
787 backpropagating APs by modulatory neurons can affect the information encoding capability of sensory
788 dendrites. The modulation of ectopic APs is independent of previous dendritic events, and can thus
789 modulate incoming sensory information without prior dendritic activation.

790 FIGURE LEGENDS

791 Figure 1. IV neuron activation decreases the frequency of ectopic spike initiation in AGR.

792 **A**, Schematic of the stomatogastric nervous system. Axonal projections of the paired IV neurons are
793 depicted in red. AGR and its axonal projections are depicted in blue. Nerve names are italicized. Green
794 circles in the CoG represent descending projection neurons. **A'**, Composite photo of AGR (yellow) and
795 STG (orange) showing the morphology of AGR and its axonal projections in the *stn* and *dgn*. AGR was
796 visualized via intracellular injection of Alexa Fluor 568. Neural structures were visualized via bath-
797 application of the voltage-sensitive dye Di-4 ANNEPS. Note that AGR possesses 1-3 arbors in the STG
798 neuropil (Städle and Stein, 2016) that are not visible here because of high background fluorescence of
799 the STG neuropil. Scale bar, 100 μ m. n=neuropil. **B**, AGR instantaneous firing frequency (AGR ff., top)
800 and extracellular nerve recordings of the *Ign* and *dgn* (bottom) showing the responses of AGR (blue) and
801 the STG gastric mill neurons before and during IV neuron stimulation (gray area). Black bars above the
802 recording visualize the repetitive stimulation of the IV neurons (40Hz, 10 consecutive trains). IV neurons
803 stimulation elicited a gastric mill rhythm (note the alternating activity of LG on the *Ign* and DG on the *dgn*)
804 and a concurrent decrease in AGR ff. by 41%. **C**, Time course of the average change in AGR ff. during 40
805 Hz IV neuron stimulation for 10 consecutive trains. AGR firing frequency was normalized to the frequency
806 measured 100 sec before IV neuron stimulation (baseline). Control refers to the frequency measured
807 immediately before the stimulation. Shown are means \pm SD. N=14 preparations. **D**, Average time course
808 of the change in normalized AGR ff. during IV neuron stimulation with varying stimulation frequency (10 to
809 50 Hz). Shown are means. N=10 preparations. Nerves: *ivn*: inferior ventricular nerve, *ion*: inferior
810 esophageal nerve, *son*: superior esophageal nerve, *dpon*: dorsal posterior esophageal nerve, *stn*:
811 stomatogastric nerve, *dgn*: dorsal gastric nerve; *agn*: anterior gastric nerve, *lvn*: lateral ventricular nerve,

812 *lgn*: lateral gastric nerve. Ganglia: STG: stomatogastric ganglion, CoG: commissural ganglion, brain:
813 supraesophageal ganglion. Neurons: AGR: anterior gastric receptor neuron, IV: inferior ventricular
814 neurons. Figure A adapted from Hedrich and Stein, 2008 and Städele et al., 2012.

815 **Figure 2. IV neuron stimulation can stop ectopic spike production.**

816 **A**, Extracellular recording of the *dgn* (bottom) and AGR instantaneous spike frequency (top) showing that
817 AGR spike amplitude changed during strong decrease of AGR instantaneous firing frequency. **A'**,
818 Magnification of the gray area in A. While AGR spikes on the *dgn* had similar shapes and amplitudes
819 before IV neuron stimulation, spike amplitude continuously changed during IV stimulation. Arrows mark
820 the changes in AGR amplitude. Ectopic APs had negative deflections and are marked blue. APs
821 generated in the periphery had positive deflections and are highlighted in green. Note the different time
822 scales in Figures A and A'. **B**, Comparison of spike appearance and delay of arrival of AGR APs with
823 negative (*Bi*) and positive deflection (*Bii*) at three recording sites along the AGR axon (*dgn*, *stn* and *son*).
824 APs on the *dgn* were used for temporal alignment. Shown are single sweeps (left, middle) and an overlay
825 of 20 APs (right) showing the loss in temporal accuracy (jitter). The recording sites where APs appeared
826 first are highlighted in bold. Colors correspond to different AP deflections as shown in A. Gray lines depict
827 the delay in AP appearance between recording sites. **C**, Example recording showing a complete stop in
828 AGR's ectopic firing during IV stimulation (gray area). Note the large gap in spike frequency after the 4th
829 IV stimulus train.

830 **Figure 3. The IV neurons exert their effects on the AGR axon via chemical transmission.**

831 **A**, AGR ff. before and during VCN stimulation (gray bar). VCN stimulation did not diminish AGR ff., but
832 started a gastric mill rhythm (see LG activity on the *lgn* and DG on the *dgn*). Recordings are from the
833 same experiment as shown in Figure 1B. **B**, Average time course of normalized AGR ff. in response to
834 VCN stimulation. Shown are mean \pm SD. VCN stimulation did not cause a significant change in AGR firing
835 frequency. N=12 preparations. **C**, AGR ff. during IV neuron stimulation in the intact nervous system (*i*),
836 after CoG transection (*ii*), and after block of chemical transmission via application of low Ca²⁺ saline to the
837 posterior *stn* (*iii*). Recordings are from the same preparation. **D**, Analysis of the average change in AGR

838 ff. during IV neuron stimulation in saline (IV stim), after CoG transection (IV stim + CoG cut), and after
 839 chemical transmission was blocked (IV stim + low Ca^{2+}). Shown are means \pm SD. Control refers to the
 840 frequency measured immediately before IV stimulation. n.s. = not significant different with $p > 0.05$, one way
 841 RM ANOVA, N=6 preparations.

842 **Figure 4. The IV neuron co-transmitter histamine diminishes the AGR firing frequency mainly via**
 843 **acting on H_2 receptors.**

844 **A-B**, AGR ff. in response to **(A)** FMRF-like peptide F1 and **(B)** histamine application to the posterior *stn*.
 845 Colored areas mark the time of drug application. Arrows in *B* indicate switches of AP initiation to other
 846 locations. **A'-B'**, Analysis of the change in AGR ff. before and during application of **(A')** FMRF-like peptide
 847 F1 and **(B')** histamine. Black circles represent individual experiments. Diamonds represent mean \pm SD.
 848 N=13 preparations. **C**, AGR ff. in response to 40 Hz IV neuron stimulation in saline (*i*), and after blocking
 849 of H_2 receptors with Cimetidine (*ii*). Recordings are from the same preparation and scaled identically. **D**,
 850 Comparison of AGR ff. during H_2 receptor blockade with cimetidine immediately before (control cimet.)
 851 and during IV stimulation (IV + cimet.). Circles represent individual experiments. Diamonds represent
 852 mean \pm SD. n.s. = not significant different, paired t-test, $t(4)=2.66$; $p=0.056$, N=5 preparations. **E**, Average
 853 change in AGR ff. in saline (gray) and cimetidine (purple). Shown are means \pm SD. One way RM ANOVA,
 854 $F(4,3)=33.27$, $p < 0.001$, Holm-Sidak post-hoc test with $p < 0.05$, N=5 preparations. n.s. = not significant
 855 different with $p=0.58$.

856 **Figure 5. IV neurons only influence AGR when APs are generated ectopically in the *stn***

857 **A-B**, Overlay of multiple AGR APs (72 APs each) for **(A)** control condition and **(B)** during HiDi application.
 858 Data are from the same preparation. Bold highlighted nerve names mark the recording site where APs
 859 appeared first. APs on the *dgn* were used for temporal alignment. **A'-B'**, Example recording showing
 860 AGR ff. before and during IV neuron stimulation for **(A')** control condition and **(B')** during HiDi application
 861 to the *stn*. Extracellular recordings of the *dgn* (bottom) show the gastric mill rhythm (rhythmic firing of DG).
 862 Data from the same preparation as shown in *A* and *B*.

863 **Figure 6. Antidromic ectopic APs alter sensory sensitivity to muscle stretch**

864 **A**, Original recordings of AGR's burst activities at different ectopic spike frequencies (7, 5, 3 Hz).
865 Recordings were taken on a section of the *dgn*. Sensory bursts were elicited by stretching the gm1
866 muscles. Ectopic APs were elicited with extracellular stimulation of the posterior part of the *stn* ('siAPs')
867 and are highlighted in light blue. Orthodromic APs of the sensory burst are depicted in green while
868 spontaneous ectopic APs are highlighted in dark blue. **B**, Overlay of several original traces from *dgn*, *stn*,
869 and *son* recordings plus average showing the directions of AP propagation for the three conditions shown
870 in A. The gray area depicts the stimulus artifact. **C - E**, Quantification of sensory bursts at siAP
871 frequencies between 3 and 10 Hz. **C**, Burst duration. **D**, Number of spikes per burst. **E**, Average intraburst
872 firing frequency. Shown are means \pm SEM. N=8 preparations.

873 **Figure 7. Antidromic ectopic APs alter sensory sensitivity to K⁺ application**

874 **A**, Original recordings of AGR's burst activities at different ectopic spike frequencies (7, 5, 3 Hz).
875 Recordings were taken on a section of the *stn*, anterior to the AGR ectopic SIZ. Sensory bursts were
876 elicited with high potassium (K⁺, arrow) in the periphery, ectopic APs with extracellular stimulation of the
877 posterior part of the *stn*. SiAPs are highlighted in light blue. Orthodromic APs of the sensory burst are
878 depicted in green while spontaneous ectopic APs are highlighted in dark blue. **B**, Overlay of several
879 original traces from *dgn*, *stn*, and *son* recordings plus average showing the directions of AP propagation
880 for the three conditions shown in A. The gray area depicts the stimulus artifact. **C - E**, Quantification of
881 sensory bursts at siAP frequencies between 3 and 10 Hz. **C**, Burst duration. **D**, Number of spikes per
882 burst. **E**, Average intraburst firing frequency. The gray area indicates the physiological range of AGR
883 firing frequency decrease during IV stimulation. Shown are means \pm SEM. N=5 preparations.

884 **Figure 8. Slow ionic conductances determine the effectiveness of ectopic APs on burst activity.**

885 **A**, Burst activity of three models with an I_{K_S} time constant of 2 sec. siAP frequency was varied from 7, to
886 5, to 3 Hz, and compared to 0 Hz (no firing). siAPs are depicted in black, sensory burst APs are
887 highlighted in green. Note that decreasing siAP firing frequency increased burst duration (gray area). For
888 better visualization, only burst starts and ends are shown. **B - D**, Analysis of changes in burst structure for

889 different I_{KS} time constants at different siAP frequencies. **B**, Burst duration. **C**, Number of spikes per burst.
890 **D**, Average intraburst firing frequency.

891 **Figure 9. IV neuron modulation does not affect en-passant AP propagation.**

892 **A**, Single burst of peripherally initiated AGR APs in response to extracellular stimulation of the *agn* with
893 28 consecutive pulses and 15 Hz stimulation frequency. Shown are spike appearances on the *dgn* (i) and
894 *son* (ii) before (black) and during IV neuron stimulation (green). APs were aligned to the stimulus and
895 plotted on top of each other so that the first spike occurs at the bottom. **B**, Comparison of spike
896 appearance for the example shown in **A**. Spike times were extracted and plotted as a function of delay to
897 the *agn* stimulation. **C**, Analysis of the temporal difference in spike appearance on the *son* before and
898 during IV stimulation for 28 consecutive APs. Δ delay is the difference in AP arrival time on the *son* during
899 IV stimulation and the no IV stimulation control. Shown are means \pm SD. N=6 preparations, n=30 APs
900 each. **D**, Example extracellular recording of the *stn* showing spike failures (arrows) of AGR APs before
901 and during IV neuron stimulation. Ectopically generated AGR spikes are highlighted in blue while *agn*
902 stimulation induced APs are depicted in black. AGR was activated in the periphery via extracellular
903 stimulation of the *agn*. Recordings are from the same preparation. **E**, Analysis of the number of spike
904 failures during 10 repetitive *agn* stimulations (40 Hz, 9 sec train/intertrain duration, 360 APs/train) before
905 (control) and during IV stimulation. Circles represent data from single experiments; diamonds represent
906 means \pm SD, N=8 preparations.

907 **REFERENCES**

- 908 Agüera y Arcas B, Fairhall AL, Bialek W (2003) Computation in a single neuron: Hodgkin and Huxley
909 revisited. *Neural Comput* 15:1715-1749.
- 910 Ausborn J, Stein W, Wolf H (2007) Frequency Control of Motor Patterning by Negative Sensory
911 Feedback. *J Neurosci* 27:9319-9328.
- 912 Baginskas A, Palani D, Chiu K, Raastad M (2009) The H-current secures action potential transmission at
913 high frequencies in rat cerebellar parallel fibers. *Eur J Neurosci* 29:87-96.
- 914 Ballo AW, Bucher D (2009) Complex intrinsic membrane properties and dopamine shape spiking activity
915 in a motor axon. *J Neurosci* 29:5062-5074.
- 916 Ballo AW, Nadim F, Bucher D (2012) Dopamine modulation of Ih improves temporal fidelity of spike
917 propagation in an unmyelinated axon. *J Neurosci* 32:5106-5119.
- 918 Ballo AW, Keene JC, Troy PJ, Goeritz ML, Nadim F, Bucher D (2010) Dopamine Modulates Ih in a Motor
919 Axon. *J Neurosci* 30:8425-8434.
- 920 Bardoni R, Takazawa T, Tong CK, Choudhury P, Scherrer G, Macdermott AB (2013) Pre- and
921 postsynaptic inhibitory control in the spinal cord dorsal horn. *Ann N Y Acad Sci* 1279:90-96.
- 922 Barriere G, Simmers J, Combes D (2008) Multiple mechanisms for integrating proprioceptive inputs that
923 converge on the same motor pattern-generating network. *J Neurosci* 28:8810-8820.
- 924 Beenhakker MP, Blitz DM, Nusbaum MP (2004) Long-lasting activation of rhythmic neuronal activity by a
925 novel mechanosensory system in the crustacean stomatogastric nervous system. *J Neurophysiol*
926 91:78-91.
- 927 Beenhakker MP, Kirby MS, Nusbaum MP (2007) Mechanosensory gating of proprioceptor input to
928 modulatory projection neurons. *J Neurosci* 27:14308-14316.
- 929 Beenhakker MP, DeLong ND, Saideman SR, Nadim F, Nusbaum MP (2005) Proprioceptor regulation of
930 motor circuit activity by presynaptic inhibition of a modulatory projection neuron. *J Neurosci* 25:8794-
931 8806.
- 932 Beloozerova IN, Rossignol S (2004) Antidromic discharges in dorsal roots of decerebrate cats. II: studies
933 during treadmill locomotion. *Brain Res* 996:227-236.
- 934 Bevengut M, Clarac F, Cattaert D (1997) Antidromic modulation of a proprioceptor sensory discharge in
935 crayfish. *J Neurophysiol* 78:1180-1183.
- 936 Birmingham JT (2001) Increasing sensor flexibility through neuromodulation. *Biol Bull* 200:206-210.

State-dependent modification of sensory sensitivity via modulation of backpropagating action potentials

- 937 Birmingham JT, Billimoria CP, DeKlotz TR, Stewart RA, Marder E (2003) Differential and history-
938 dependent modulation of a stretch receptor in the stomatogastric system of the crab, *Cancer borealis*.
939 J Neurophysiol 90:3608-3616.
- 940 Blitz DM, Nusbaum MP (2011) Neural circuit flexibility in a small sensorimotor system. Curr Opin
941 Neurobiol 21:544-552.
- 942 Böhm H, Dybek E, Heinzel HG (2001) Anatomy and in vivo activity of neurons connecting the crustacean
943 stomatogastric nervous system to the brain. Journal of Comparative Physiology A Sensory Neural and
944 Behavioral Physiology 187:393-403.
- 945 Bostock H, Grafe P (1985) Activity-dependent excitability changes in normal and demyelinated rat spinal
946 root axons. J Physiol 365:239-257.
- 947 Brozski TJ, Bauer CA (2016) Animal models of tinnitus. Hear Res 338:88-97.
- 948 Bucher D, Goillard J-M (2011) Beyond faithful conduction: short-term dynamics, neuromodulation, and
949 long-term regulation of spike propagation in the axon. Prog Neurobiol 94:307-346.
- 950 Bucher D, Thirumalai V, Marder E (2003) Axonal dopamine receptors activate peripheral spike initiation in
951 a stomatogastric motor neuron. J Neurosci 23:6866-6875.
- 952 Bukalo O, Campanac E, Hoffman DA, Fields RD (2013) Synaptic plasticity by antidromic firing during
953 hippocampal network oscillations. Proc Natl Acad Sci U S A 110:5175-5180.
- 954 Burrows M, Matheson T (1994) A presynaptic gain control mechanism among sensory neurons of a locust
955 leg proprioceptor. J Neurosci 14:272-282.
- 956 Cattaert D, El Manira A, Bevengut M (1999) Presynaptic inhibition and antidromic discharges in crayfish
957 primary afferents. J Physiol Paris 93:349-358.
- 958 Cebada J, Garcia U (2007) Histamine operates Cl⁻-gated channels in crayfish neurosecretory cells. J Exp
959 Biol 210:3962-3969.
- 960 Christie AE, Stein W, Quinlan JE, Beenhakker MP, Marder E, Nusbaum MP (2004) Actions of a
961 histaminergic/peptidergic projection neuron on rhythmic motor patterns in the stomatogastric nervous
962 system of the crab *Cancer borealis*. J Comp Neurol 469:153-169.
- 963 Claiborne BJ, Selverston AI (1984) Histamine as a neurotransmitter in the stomatogastric nervous system
964 of the spiny lobster. J Neurosci 4:708-721.
- 965 Clarac F, Cattaert D (1996) Invertebrate presynaptic inhibition and motor control. Exp Brain Res 112:163-
966 180.
- 967 Coleman MJ, Meyrand P, Nusbaum MP (1995) A switch between two modes of synaptic transmission
968 mediated by presynaptic inhibition. Nature 378:502-505.

State-dependent modification of sensory sensitivity via modulation of backpropagating action potentials

- 969 Combes D, Simmers J, Moulins M (1995) Structural and functional characterization of a muscle tendon
970 proprioceptor in lobster. *J Comp Neurol* 363:221-234.
- 971 Combes D, Simmers J, Nonnotte L, Moulins M (1993) Tetrodotoxin-sensitive dendritic spiking and control
972 of axonal firing in a lobster mechanoreceptor neurone. *J Physiol* 460:581-602.
- 973 Cropper EC, Evans CG, Jing J, Klein A, Proekt A, Romero A, Rosen SC (2004) Regulation of afferent
974 transmission in the feeding circuitry of *Aplysia*. *Acta Biol Hung* 55:211-220.
- 975 Daur N, Nadim F, Stein W (2009) Regulation of motor patterns by the central spike-initiation zone of a
976 sensory neuron. *Eur J Neurosci* 30:808-822.
- 977 Daur N, Diehl F, Mader W, Stein W (2012) The stomatogastric nervous system as a model for studying
978 sensorimotor interactions in real-time closed-loop conditions. *Front Comp Neurosci* 6.
- 979 Davis M (1980) Neurochemical modulation of sensory-motor reactivity: acoustic and tactile startle
980 reflexes. *Neurosci Biobehav Rev* 4:241-263.
- 981 Debanne D (2004) Information processing in the axon. *Nat Rev Neurosci* 5:304-316.
- 982 DeLong ND, Beenhakker MP, Nusbaum MP (2009) Presynaptic inhibition selectively weakens peptidergic
983 cotransmission in a small motor system. *J Neurophysiol* 102:3492-3504.
- 984 DeMaegd ML, Stein W (2018) Long-Distance Modulation of Sensory Encoding via Axonal
985 Neuromodulation. In: *Sensory Nervous System* (Heinbockel T, ed). Rijeka: InTech Open.
- 986 DeMaegd ML, Städele C, Stein W (2017) Axonal Conduction Velocity Measurement. *Bio-protocol*
987 7:e2152.
- 988 Dickinson PS (2006) Neuromodulation of central pattern generators in invertebrates and vertebrates. *Curr*
989 *Opin Neurobiol* 16:604-614.
- 990 Dubuc R, Cabelguen JM, Rossignol S (1988) Rhythmic fluctuations of dorsal root potentials and
991 antidromic discharges of primary afferents during fictive locomotion in the cat. *J Neurophysiol* 60:2014-
992 2036.
- 993 Dugladze T, Schmitz D, Whittington MA, Vida I, Gloveli T (2012) Segregation of axonal and somatic
994 activity during fast network oscillations. *Science* 336:1458-1461.
- 995 Ekeberg Ö, Wallén P, Lansner A, Travén H, Brodin L, Grillner S (1991) A computer based model for
996 realistic simulations of neural networks. *Biol Cybern* 65:81-90.
- 997 El Manira A, Clarac F (1994) Presynaptic inhibition is mediated by histamine and GABA in the crustacean
998 escape reaction. *J Neurophysiol* 71:1088-1095.
- 999 Evans CG, Jing J, Rosen SC, Cropper EC (2003) Regulation of Spike Initiation and Propagation in an
1000 *Aplysia* Sensory Neuron: Gating-In via Central Depolarization. *J Neurosci* 23:2920-2931.

State-dependent modification of sensory sensitivity via modulation of backpropagating action potentials

- 1001 Garcia L, D'Alessandro G, Fernagut PO, Bioulac B, Hammond C (2005) Impact of high-frequency
1002 stimulation parameters on the pattern of discharge of subthalamic neurons. *J Neurophysiol* 94:3662-
1003 3669.
- 1004 Goaillard JM, Schulz DJ, Kilman VL, Marder E (2004) Octopamine modulates the axons of modulatory
1005 projection neurons. *J Neurosci* 24:7063-7073.
- 1006 Goldsmith CJ, Städele C, Stein W (2014) Optical imaging of neuronal activity and visualization of fine
1007 neural structures in non-desheathed nervous systems. *PLoS ONE* 9:e103459.
- 1008 Grafe P, Quasthoff S, Grosskreutz J, Alzheimer C (1997) Function of the hyperpolarization-activated
1009 inward rectification in nonmyelinated peripheral rat and human axons. *J Neurophysiol* 77:421-426.
- 1010 Grossman Y, Parnas I, Spira ME (1979) Differential conduction block in branches of a bifurcating axon. *J*
1011 *Physiol* 295:283-305.
- 1012 Haas HL, Konnerth A (1983) Histamine and noradrenaline decrease calcium-activated potassium
1013 conductance in hippocampal pyramidal cells. *Nature* 302:432-434.
- 1014 Haas HL, Sergeeva OA, Selbach O (2008) Histamine in the nervous system. *Physiol Rev* 88:1183-1241.
- 1015 Hatton GI, Yang QZ (2001) Ionotropic histamine receptors and H2 receptors modulate supraoptic
1016 oxytocin neuronal excitability and dye coupling. *J Neurosci* 21:2974-2982.
- 1017 Hedrich UB, Stein W (2008) Characterization of a descending pathway: activation and effects on motor
1018 patterns in the brachyuran crustacean stomatogastric nervous system. *J Exp Biol* 211:2624-2637.
- 1019 Hedrich UB, Smarandache CR, Stein W (2009) Differential activation of projection neurons by two
1020 sensory pathways contributes to motor pattern selection. *J Neurophysiol* 102:2866-2879.
- 1021 Hedrich UB, Diehl F, Stein W (2011) Gastric and pyloric motor pattern control by a modulatory projection
1022 neuron in the intact crab *Cancer pagurus*. *J Neurophysiol* 105:1671-1680.
- 1023 Hoke KL, Pitts NL (2012) Modulation of sensory-motor integration as a general mechanism for context
1024 dependence of behavior. *Gen Comp Endocrinol* 176:465-471.
- 1025 Katz PS, Frost WN (1996) Intrinsic neuromodulation: altering neuronal circuits from within. *Trends*
1026 *Neurosci* 19:54-61.
- 1027 Kawai F, Kurahashi T, Kaneko A (1999) Adrenaline enhances odorant contrast by modulating signal
1028 encoding in olfactory receptor cells. *Nat Neurosci* 2:133-138.
- 1029 Krnjevic K, Miledi R (1959) Presynaptic failure of neuromuscular propagation in rats. *J Physiol* 149:1-22.
- 1030 Lambe EK, Picciotto MR, Aghajanian GK (2003) Nicotine induces glutamate release from thalamocortical
1031 terminals in prefrontal cortex. *Neuropsychopharmacology* 28:216-225.

State-dependent modification of sensory sensitivity via modulation of backpropagating action potentials

- 1032 Lang PM, Moalem-Taylor G, Tracey DJ, Bostock H, Grafe P (2006) Activity-dependent modulation of
1033 axonal excitability in unmyelinated peripheral rat nerve fibers by the 5-HT(3) serotonin receptor. J
1034 Neurophysiol 96:2963-2971.
- 1035 Lee AH, Megalou EV, Wang J, Frost WN (2012) Axonal conduction block as a novel mechanism of
1036 prepulse inhibition. J Neurosci 32:15262-15270.
- 1037 Lee KH, Broberger C, Kim U, McCormick DA (2004) Histamine modulates thalamocortical activity by
1038 activating a chloride conductance in ferret perigeniculate neurons. Proc Natl Acad Sci U S A
1039 101:6716-6721.
- 1040 Lemon CH (2017) Modulation of taste processing by temperature. Am J Physiol Regul Integr Comp
1041 Physiol 313:R305-R321.
- 1042 Lena C, Changeux JP, Mulle C (1993) Evidence for "preterminal" nicotinic receptors on GABAergic axons
1043 in the rat interpeduncular nucleus. J Neurosci 13:2680-2688.
- 1044 Li D, Yang H, Meyerson BA, Linderoth B (2006) Response to spinal cord stimulation in variants of the
1045 spared nerve injury pain model. Neurosci Lett 400:115-120.
- 1046 Li L, Pulver SR, Kelley WP, Thirumalai V, Sweedler JV, Marder E (2002) Orcokinin peptides in developing
1047 and adult crustacean stomatogastric nervous systems and pericardial organs. J Comp Neurol
1048 444:227-244.
- 1049 Ma C, LaMotte RH (2007) Multiple sites for generation of ectopic spontaneous activity in neurons of the
1050 chronically compressed dorsal root ganglion. J Neurosci 27:14059-14068.
- 1051 Marder E, Bucher D (2001) Central pattern generators and the control of rhythmic movements. Curr Biol
1052 11:R986-996.
- 1053 Margrie TW, Sakmann B, Urban NN (2001) Action potential propagation in mitral cell lateral dendrites is
1054 decremental and controls recurrent and lateral inhibition in the mammalian olfactory bulb. Proc Natl
1055 Acad Sci U S A 98:319-324.
- 1056 Markram H, Lubke J, Frotscher M, Sakmann B (1997) Regulation of synaptic efficacy by coincidence of
1057 postsynaptic APs and EPSPs. Science 275:213-215.
- 1058 McCormick DA, Williamson A (1991) Modulation of neuronal firing mode in cat and guinea pig LGNd by
1059 histamine: possible cellular mechanisms of histaminergic control of arousal. J Neurosci 11:3188-3199.
- 1060 Meyrand P, Weimann JM, Marder E (1992) Multiple axonal spike initiation zones in a motor neuron:
1061 serotonin activation. J Neurosci 12:2803-2812.
- 1062 Mitchell GS, Johnson SM (2003) Neuroplasticity in respiratory motor control. J Appl Physiol 94:358-374.
- 1063 Moalem-Taylor G, Lang PM, Tracey DJ, Grafe P (2007) Post-spike excitability indicates changes in
1064 membrane potential of isolated C-fibers. Muscle Nerve 36:172-182.

- 1065 Nadim F, Bucher D (2014) Neuromodulation of neurons and synapses. *Curr Opin Neurobiol* 29C:48-56.
- 1066 Nusbaum MP (2013) Modulatory Projection Neurons. In: *Encyclopedia of Neuroscience* (Binder MD,
1067 Hirokawa, N., Windhorst, U., ed): Springer, Berlin, Heidelberg.
- 1068 Nusbaum MP, Blitz DM, Marder E (2017) Functional consequences of neuropeptide and small-molecule
1069 co-transmission. *Nat Rev Neurosci* 18:389-403.
- 1070 Panzeri S, Petersen RS, Schultz SR, Lebedev M, Diamond ME (2001) The role of spike timing in the
1071 coding of stimulus location in rat somatosensory cortex. *Neuron* 29:769-777.
- 1072 Papatheodoropoulos C (2008) A possible role of ectopic action potentials in the *in vitro* hippocampal
1073 sharp wave-ripple complexes. *Neuroscience* 157:495-501.
- 1074 Pedarzani P, Storm JF (1993) PKA mediates the effects of monoamine transmitters on the K⁺ current
1075 underlying the slow spike frequency adaptation in hippocampal neurons. *Neuron* 11:1023-1035.
- 1076 Pedarzani P, Storm JF (1995) Protein kinase A-independent modulation of ion channels in the brain by
1077 cyclic AMP. *Proc Natl Acad Sci U S A* 92:11716-11720.
- 1078 Pinault D (1995) Backpropagation of action potentials generated at ectopic axonal loci: hypothesis that
1079 axon terminals integrate local environmental signals. *Brain Res Rev* 21:42-92.
- 1080 Pulver SR, Thirumalai V, Richards KS, Marder E (2003) Dopamine and histamine in the developing
1081 stomatogastric system of the lobster *Homarus americanus*. *J Comp Neurol* 462:400-414.
- 1082 Sasaki T, Matsuki N, Ikegaya Y (2011) Action-potential modulation during axonal conduction. *Science*
1083 331:599-601.
- 1084 Sauer AE, Buschges A, Stein W (1997) Role of presynaptic inputs to proprioceptive afferents in tuning
1085 sensorimotor pathways of an insect joint control network. *J Neurobiol* 32:359-376.
- 1086 Schmitz J, Stein W (2000) Convergence of load and movement information onto leg motoneurons in
1087 insects. *J Neurobiol* 42:424-436.
- 1088 Selverston AI, Szucs A, Huerta R, Pinto R, Reyes M (2009) Neural mechanisms underlying the
1089 generation of the lobster gastric mill motor pattern. *Front Neural Circuits* 3:12-12.
- 1090 Smarandache CR, Stein W (2007) Sensory-induced modification of two motor patterns in the crab,
1091 *Cancer pagurus*. *J Exp Biol* 210:2912-2922.
- 1092 Smarandache CR, Daur N, Hedrich UB, Stein W (2008) Regulation of motor pattern frequency by
1093 reversals in proprioceptive feedback. *Eur J Neurosci* 28:460-474.
- 1094 Soleng AF, Chiu K, Raastad M (2003) Unmyelinated axons in the rat hippocampus hyperpolarize and
1095 activate an H current when spike frequency exceeds 1 Hz. *J Physiol* 552:459-470.

State-dependent modification of sensory sensitivity via modulation of backpropagating action potentials

- 1096 Städele C, Stein W (2016) The Site of Spontaneous Ectopic Spike Initiation Facilitates Signal Integration
1097 in a Sensory Neuron. *J Neurosci* 36:6718-6731.
- 1098 Städele C, Andras P, Stein W (2012) Simultaneous measurement of membrane potential changes in
1099 multiple pattern generating neurons using voltage sensitive dye imaging. *J Neurosci Methods* 203:78-
1100 88.
- 1101 Städele C, Heigele S, Stein W (2015) Neuromodulation to the Rescue: Compensation of Temperature-
1102 Induced Breakdown of Rhythmic Motor Patterns via Extrinsic Neuromodulatory Input. *PLoS Biol*
1103 13:e1002265.
- 1104 Städele C, DeMaegd ML, Stein W (2017) Extracellular Axon Stimulation. *Bio-protocol* 7:e2151.
- 1105 Stein W (2009) Modulation of stomatogastric rhythms. *J Comp Physiol A* 195:989-1009.
- 1106 Stein W (2017) Stomatogastric Nervous System. In: *Oxford Research Encyclopedia*,
1107 <http://dx.doi.org/10.1093/acrefore/9780190264086.013.153>: Oxford University Press.
- 1108 Stein W, Schmitz J (1999) Multimodal convergence of presynaptic afferent inhibition in insect
1109 proprioceptors. *J Neurophysiol* 82:512-514.
- 1110 Stein W, Ausborn J (2004) Analog modulation of digital computation in nerve cells: Simulating the
1111 stomatogastric nervous system of the crab. In: *Eurosis-ETI Mod Sim*, pp 148-152. Ghent Belgium.
- 1112 Stein W, Städele C, Smarandache-Wellmann CR (2016) Evolutionary aspects of motor control and
1113 coordination: the central pattern generators in the crustacean stomatogastric and swimmeret systems.
1114 In: *Structure and evolution of invertebrate nervous systems*. (Schmidt-Rhaesa A, Harzsch S, Purschke
1115 G, eds): Oxford University Press.
- 1116 Stein W, DeLong ND, Wood DE, Nusbaum MP (2007) Divergent co-transmitter actions underlie motor
1117 pattern activation by a modulatory projection neuron. *Eur J Neurosci* 26:1148-1165.
- 1118 Straub O, Mader W, Ausborn J, Stein W (2004) Motor output variability in a joint control system - a
1119 simulation study. In: *Eurosis-ETI Mod Sim*, pp 135-139. Ghent Belgium.
- 1120 Tsuda M (2017) Modulation of Pain and Itch by Spinal Glia. *Neurosci Bull*:1-8.
- 1121 Waters J, Schaefer A, Sakmann B (2005) Backpropagating action potentials in neurones: measurement,
1122 mechanisms and potential functions. *Prog Biophys Mol Biol* 87:145-170.
- 1123 Wu YW, Grebenyuk S, McHugh TJ, Rusakov DA, Semyanov A (2012) Backpropagating action potentials
1124 enable detection of extrasynaptic glutamate by NMDA receptors. *Cell Rep* 1:495-505.
- 1125 Xiong W, Chen WR (2002) Dynamic gating of spike propagation in the mitral cell lateral dendrites. *Neuron*
1126 34:115-126.

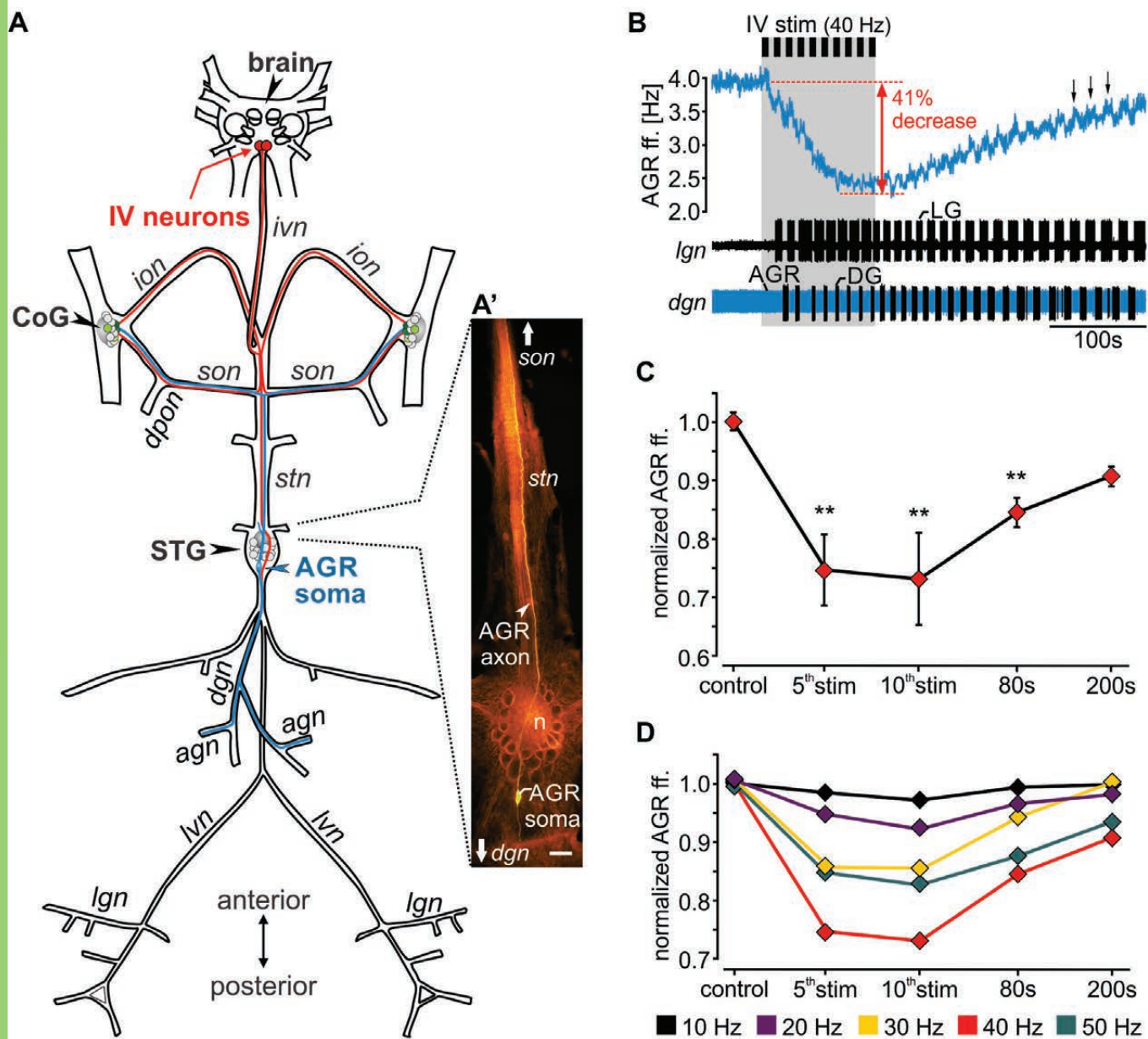
State-dependent modification of sensory sensitivity via modulation of backpropagating action potentials

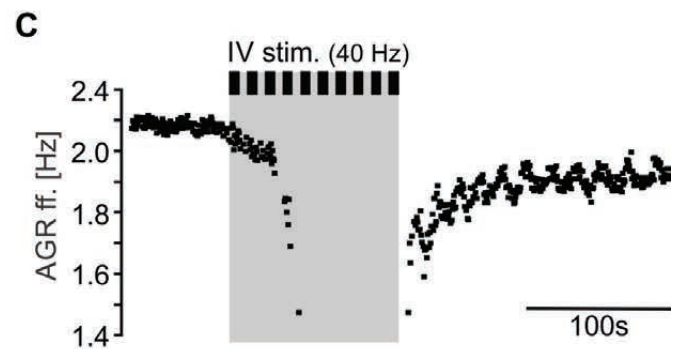
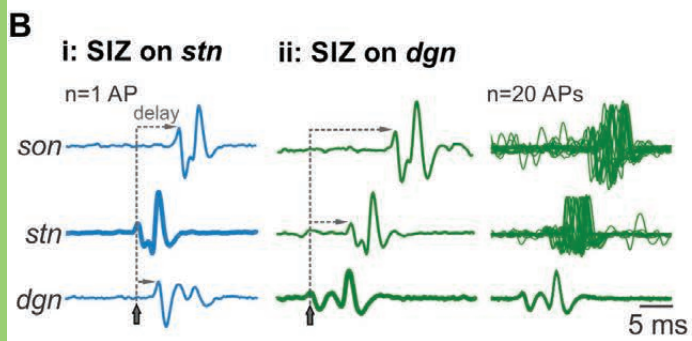
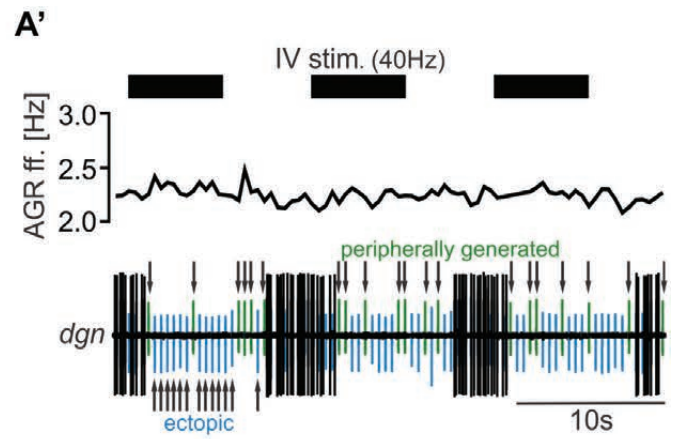
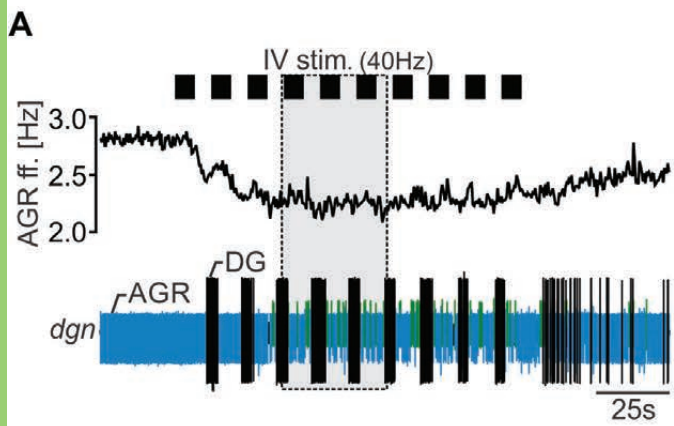
- 1127 Zhang Y, Bucher D, Nadim F (2017) Ionic mechanisms underlying history-dependence of conduction
1128 delay in an unmyelinated axon. eLife 6:e25382.

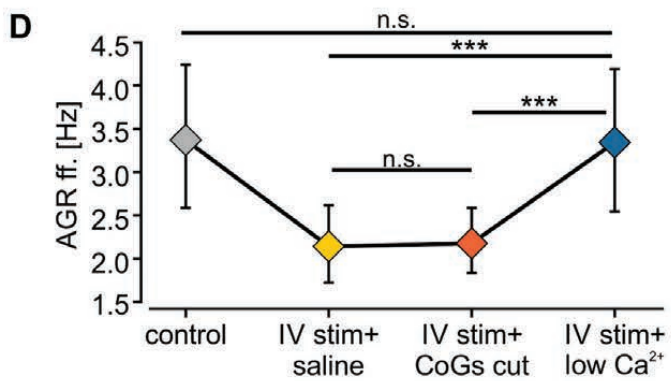
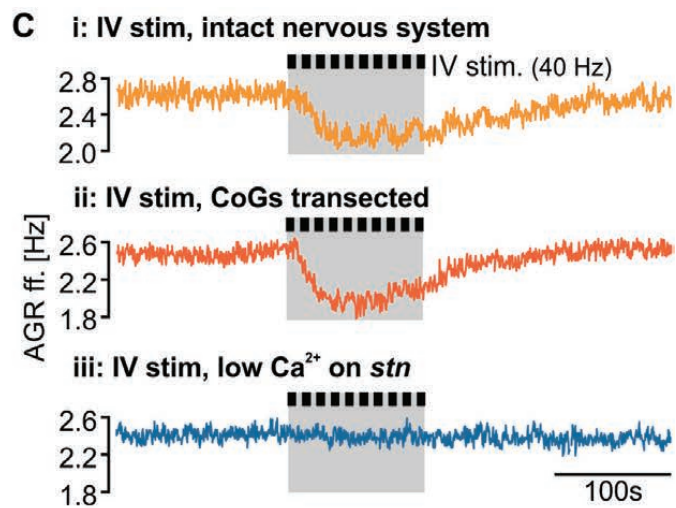
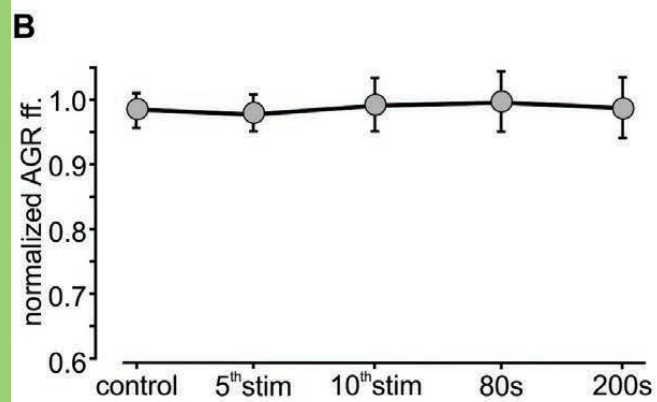
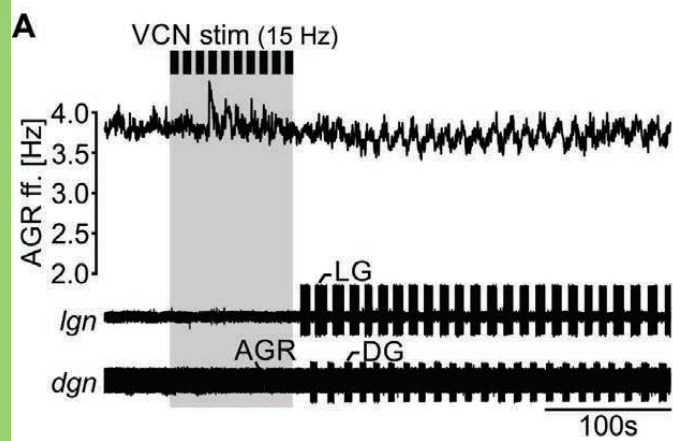
Table 1. Statistical Tests Summary

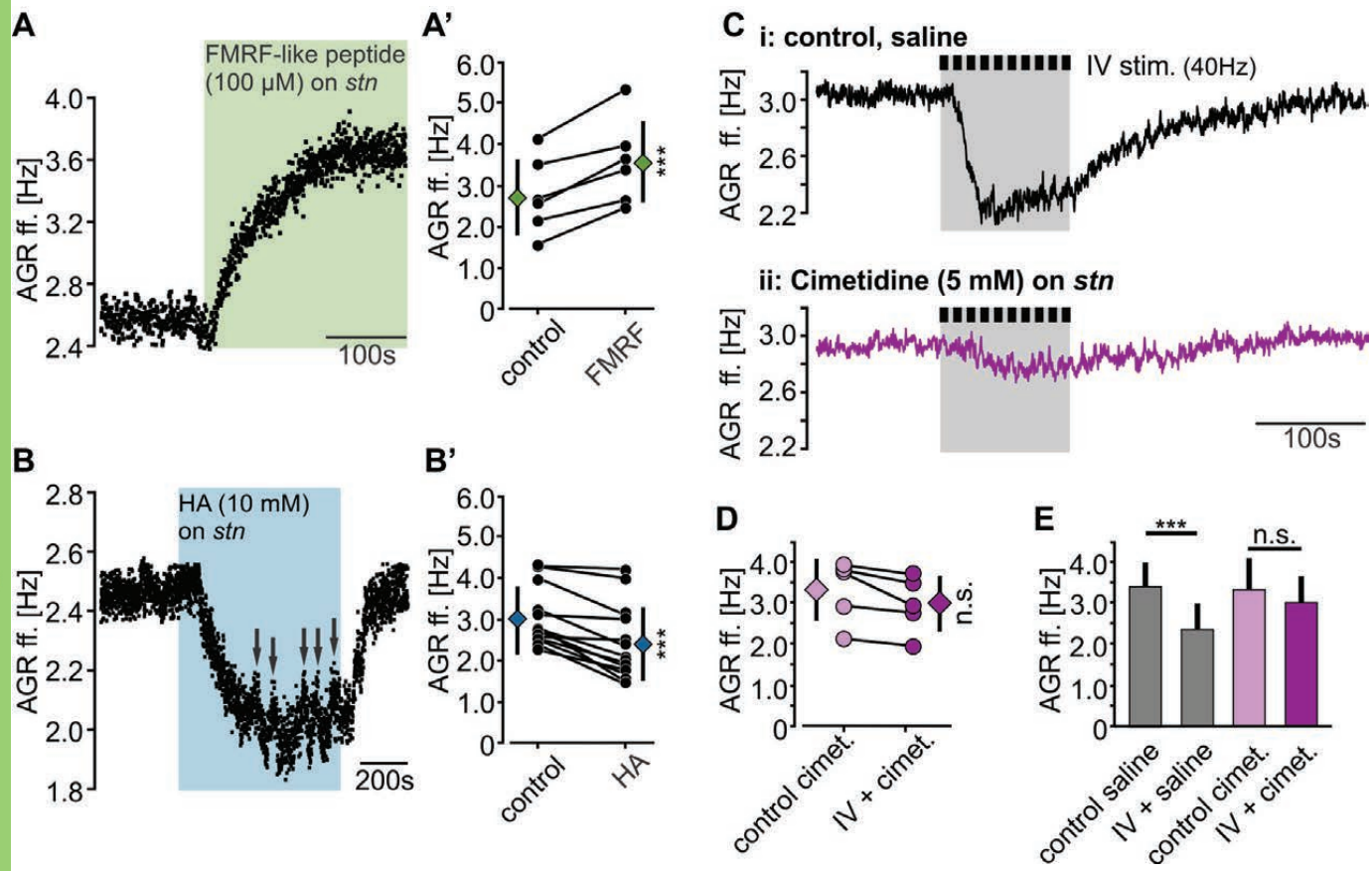
Figure	Data structure	Type of test	Output	p value
1C	Normal	One way RM ANOVA, Holm-Sidak post-hoc test	F(13,4)=49.21	p<0.001 (ANOVA) p<0.05 (post hoc)
1D	Normal	One way RM ANOVA, Holm-Sidak post-hoc test	F(4,4)=49.21	p<0.001 (ANOVA) p<0.01 (post hoc)
3B	Normal	One way RM ANOVA	F(11,4)=4.17	p=0.06
3D	Normal	One way RM ANOVA, Holm-Sidak post-hoc test	F(3,17)=32.36	p<0.001 (ANOVA) p<0.01 (post hoc)
4A	Normal	Paired t-test	N/A	p=0.001
4B	Normal	Paired t-test	N/A	p=0.001
4D	Normal	Paired t-test	N/A	p=0.056
6C	Normal	One way RM ANOVA, Student- Newman-Keuls post-hoc test	F(7,42)=3.831	p=0.003 (ANOVA) p<0.05 (post hoc)
6D	Normal	One way RM ANOVA, Student- Newman-Keuls post-hoc test	F(7,42)=9.717	p=0.003 (ANOVA)

				p<0.05 (post hoc)
6E	Normal	One way RM ANOVA	F(9,56)=1.198	p=0.315
7C	Normal	One way RM ANOVA, Student-Newman-Keuls post-hoc test	F(4,28)=4.65	p=0.001 (ANOVA) p<0.05 (post hoc)
7D	Normal	One way RM ANOVA, Student-Newman-Keuls post-hoc test	F(4,28)=3.29	p=0.038 (ANOVA) p<0.05 (post hoc)
7E	Normal	One way RM ANOVA	F(4,28)=1.07	p=0.15
9C	Normal	Paired t-test	N/A	p=0.38
9E	Normal	Paired t-test	N/A	p=0.5

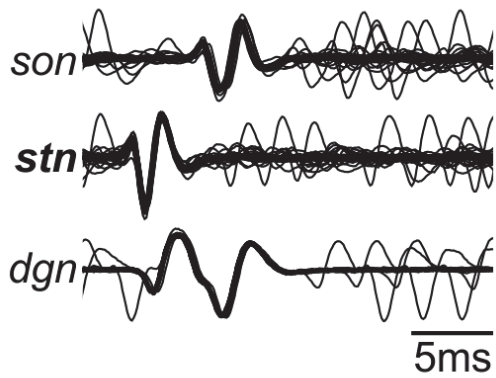




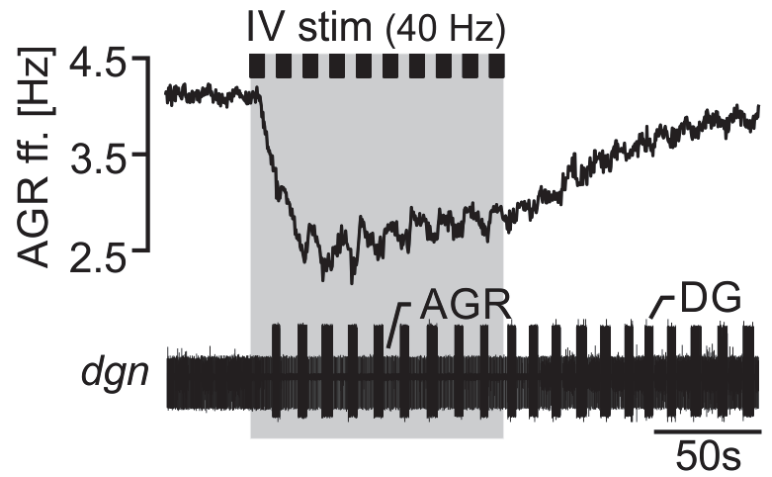




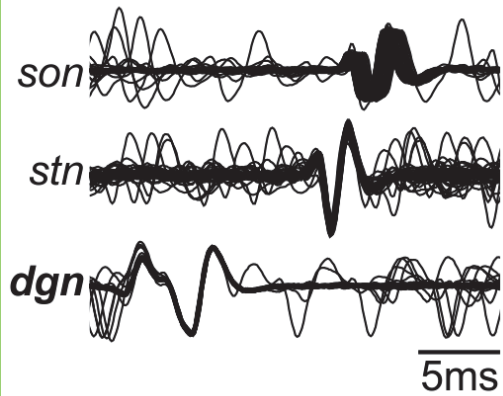
A control



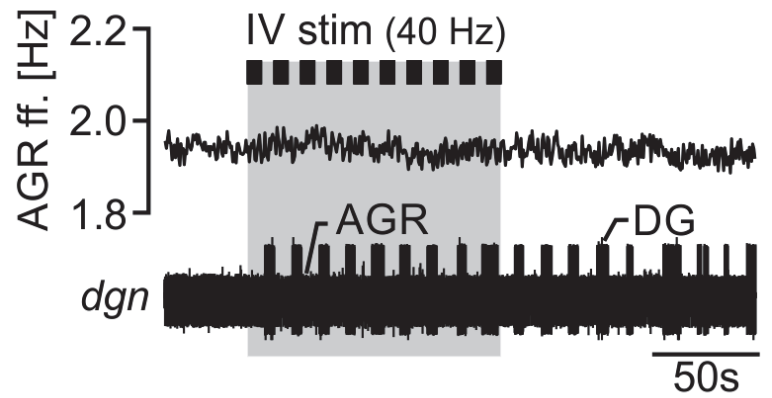
A' control

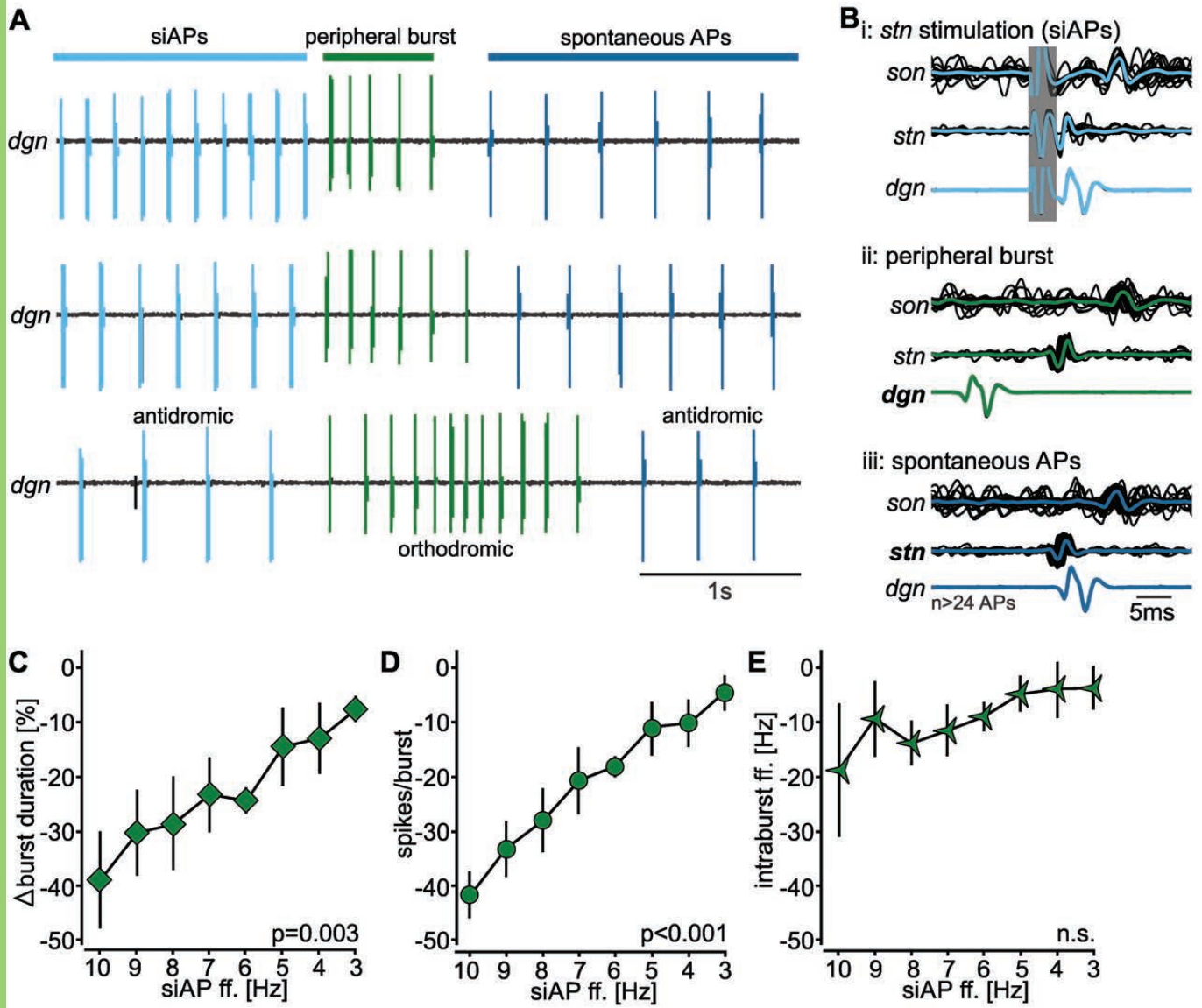


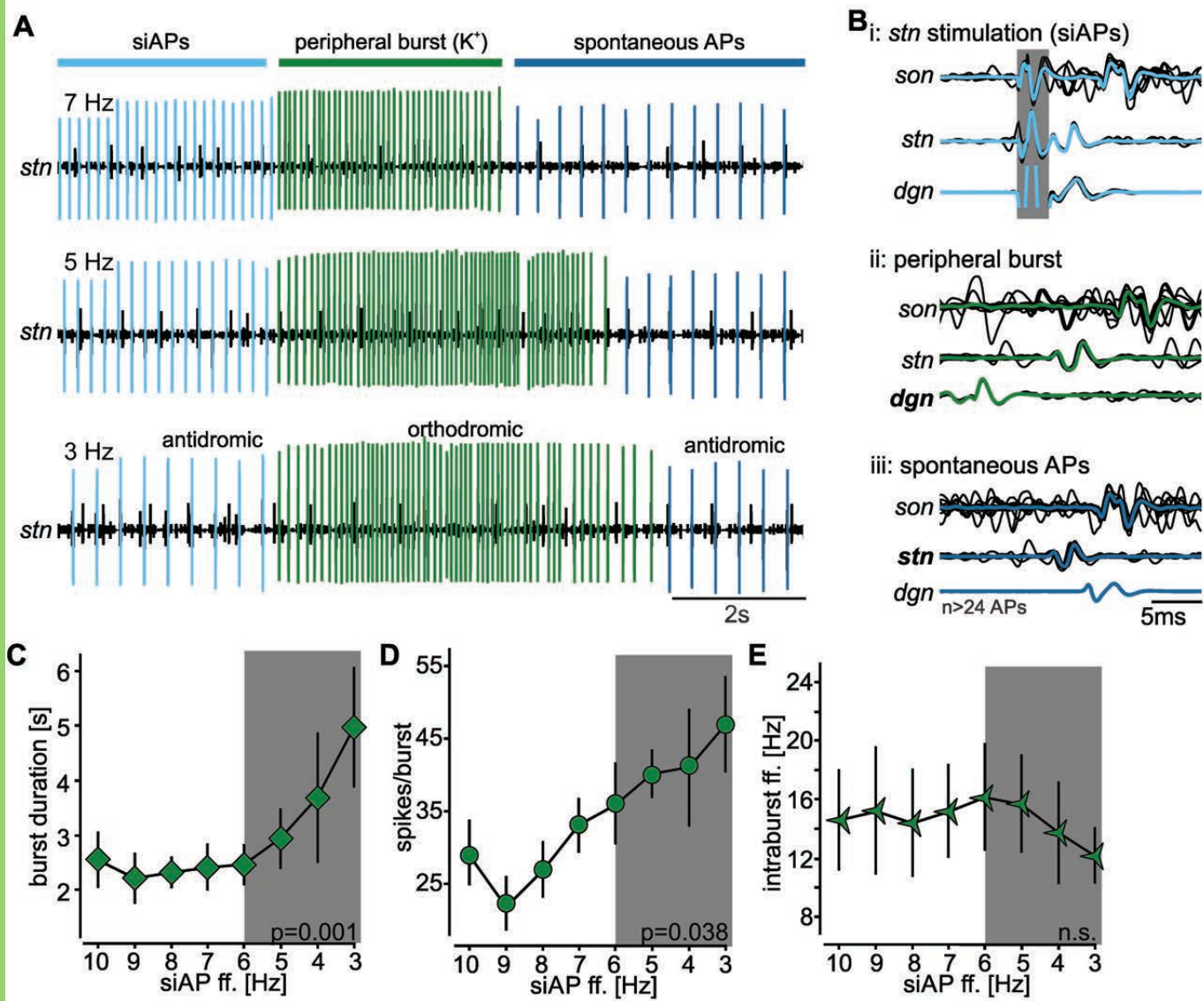
B HiDi on *stn*

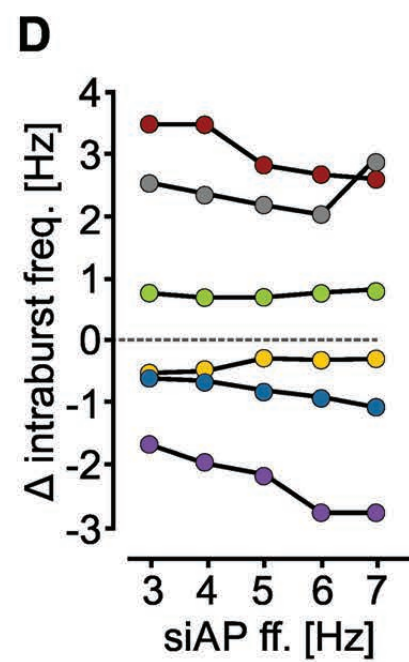
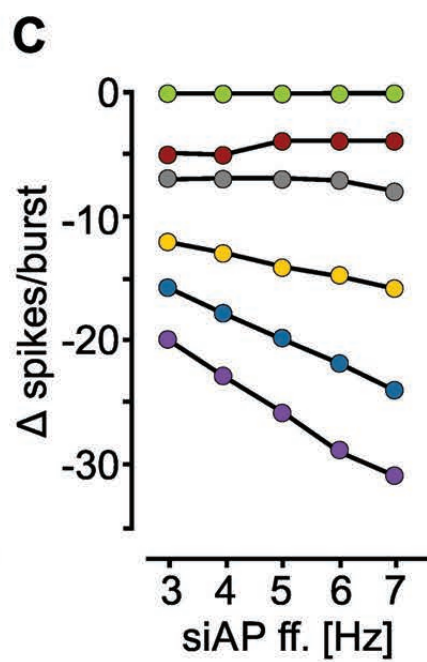
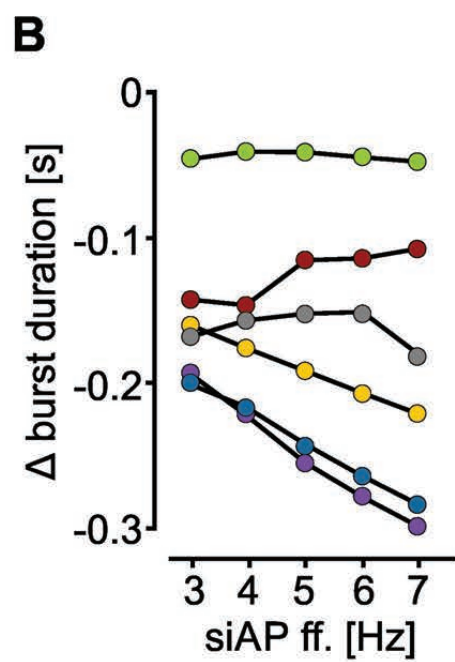
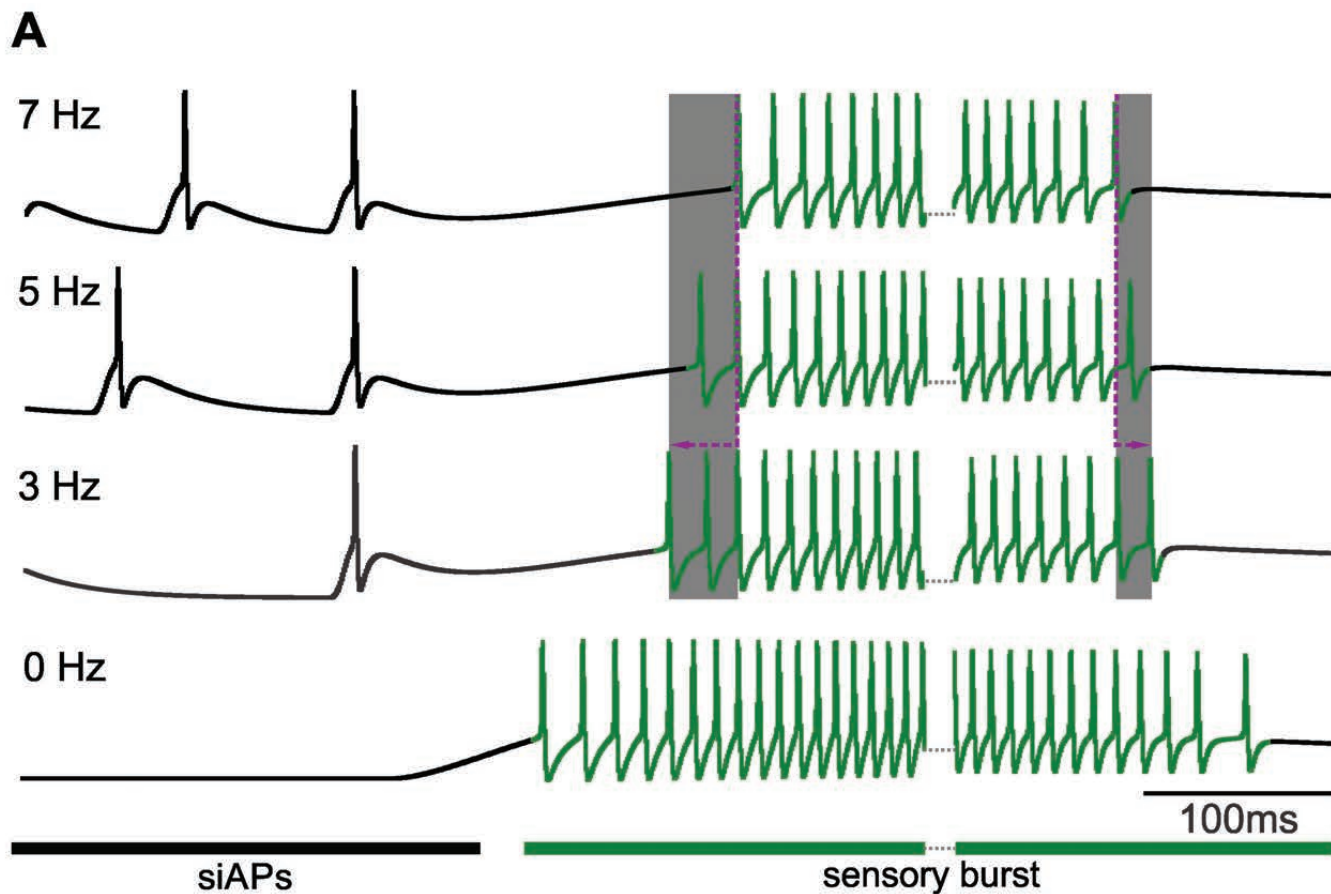


B'









● no I_{ks} ● $\tau = 0.25s$ ● $\tau = 0.5s$ ● $\tau = 1s$ ● $\tau = 2s$ ● $\tau = 4s$

